GENERAL MOTORS CORPORATION

INVESTIGATION OF THE REACTION OF THE LUNAR SURFACE TO THE IMPACT OF A LUNAR PROBE

FACILITY FORM 602

N65-31060 (ACCESSION NUMBER)

(THRU)

62 (PAGES)

1 (CODE)

CR 64363 (NASA CR OR TMX OR AD NUMBER)

30 (CATEGORY)

FINAL REPORT

CONTRACT NO. JPL 950299

JET PROPULSION LABORATORY

CALIFORNIA INSTITUTE OF TECHNOLOGY

GM DEFENSE RESEARCH LABORATORIES

SANTA BARBARA, CALIFORNIA

AEROSPACE OPERATIONS DEPARTMENT

GPO PRICE $ _____

CFSTI PRICE(S) $ _____

Hard copy (HC) 3.00

Microfiche (MF) .75

ff 653 July 65

TR63-215

JUNE 1963

RQT-20313

Copy No 68

GENERAL MOTORS CORPORATION

INVESTIGATION OF THE REACTION OF THE LUNAR SURFACE TO THE IMPACT OF A LUNAR PROBE

PREPARED BY

J.W. GEHRING

R.L. WARNICA

FINAL REPORT

CONTRACT NO. JPL 950299

JET PROPULSION LABORATORY

CALIFORNIA INSTITUTE OF TECHNOLOGY

GM DEFENSE RESEARCH LABORATORIES

SANTA BARBARA, CALIFORNIA

AEROSPACE OPERATIONS DEPARTMENT

TR63-215

JUNE 1963

CONTENTS

Section		Page
I	Scope of Research Program	1
	Approach to Research Program	2
II	Range and Monitoring Instrumentation	6
III	Results and Analysis	18
	Observations of the Impact Flash and Target Crater	21
	Effect of Ambient Gas and Pressure	21
	Effects of Varied Projectile Parameters and Target Material	25
	Duration of Impact Flash	38
	Spectrum of an Impact Flash	42
IV	Discussion of Experimental Results	47
	Observations of Lunar Impact	48
V	Conclusions	55
VI	References	57

ILLUSTRATIONS

Figure		Page
1	Schematic of Ballistics Range "A"	7
2	The 0.22-Caliber Accelerated-Reservoir Light-Gas Gun – Ballistics Range "A"	8
3	The 0.22-Inch SuperSwift Smoothbore Rifle – Ballistics Range "A"	9
4	Summary of Launcher Performance	10
5	Ballistics Range "C (vertical)	11
6	Velocity and Impact Chambers – Ballistics Range "A"	13
7	Schematic of Ballistics Range Velocity Station	14
8	Typical Shadowgraph Showing Separation of Model and Sabot	15
9	Spectrograph Optical Train Installation	17
10	Typical Impact Flash in Sand (Nevada 135)	22
11	Typical Impact Craters Formed in Sand and Rock	23
12	Effects of Velocity and Pressure on Peak Luminosity from Impact of Nylon Spheres (0.22-In. Diam) on Sand Targets (Nevada 135)	24
13	Reduced Data – Variation of Peak Luminosity with Pressure for Nylon Spheres (0.22-In. Diam) Impacting Sand and Aluminum at 8,000 fps in Air and Helium	26
14	Effect of Velocity on Peak Luminosity for Glass and Aluminum Spheres Impacting Sand Targets (Nevada 135)	28
15	Effect of Velocity on Peak Luminosity of Aluminum Spheres (1/8-In. Diam) Impacting Sand and Granite	29

ILLUSTRATIONS (continued)

Figure		Page
16	Effect of Velocity on Peak Luminosity for Nylon Spheres (0.22-In.Diam) Impacting Aluminum Targets	30
17	Effects of Velocity and Projectile Diameter on Peak Luminosity for Steel Spheres of Various Sizes Impacting Sand Targets (Nevada 135)	31
18	Reduced Data – Variation of Peak Luminosity with Projectile Diameter (Velocity = 8,000 fps)	33
19	Reduced Data – Variation of Peak Luminosity with Projectile Mass (Diameter = Constant = 1/8 Inch; Velocity = 8,000 fps; Target of 1100F Aluminum)	34
20	Effect of Velocity on Peak Luminosity from Impact of Nylon Spheres (0.22-In. Diam) Impacting Various Basalt Targets	36
21	Typical Photomultiplier Traces from Impacts of Various Projectile-Target Combinations	40
22	Sequential Beckman-Whitley Photographs of a 1/8-In. Glass Sphere Impacting an Aluminum Target at 23,000 ft/sec	43
23	Spectrogram of Impact Flash Generated by Nylon Cylinder Impacting an Aluminum Target at 24,600 ft/sec	44
24	Spectrogram of Impact Flash Generated by Nylon Spheres Impacting Sand Targets at Approximately 10,000 ft/sec (10 rounds superimposed)	45

SECTION I

SCOPE OF RESEARCH PROGRAM

HBST

31060

This paper presents the results of an experimental research program to investigate the flash phenomena associated with high velocity impact. Specifically, the program was directed toward obtaining basic data about impact flash phenomena and using this data, together with that obtained from impacts on simulated lunar surfaces, to estimate the characteristics of the flash from the impact of a lunar probe on the moon.

The program consisted of a parametric study of the variables associated with impacting a projectile against various targets, some of which simulate the lunar surface. The tests consisted of firing projectiles of varied mass, material, and velocity into a variety of target materials. Observations were made and quantitative data obtained for the magnitude of the luminosity of the impact flash, the duration of the flash, and the spectrum of emitted light. Also, high-speed optical pictures were made to determine the disposition of the impacting projectile and of the debris ejected from the resultant crater. From analysis of the experimental data, it is possible to make an estimate of the impact flash likely to be observed upon impact of a lunar probe with the moon's surface and the possibility of observing the flash from the earth.

APPROACH TO RESEARCH PROGRAM

The research program to be described in this paper was directed toward the possibility of identifying the impact of a lunar probe on the lunar surface and the techniques required for identification of the lunar surface material. The program, therefore, was conducted with the specific goal of permitting recommendations to be made as to the observations and techniques which can be carried out from a remote position to answer the important questions related to lunar impact phenomena.

When a lunar probe strikes the moon's surface it will (1) generate an intense flash of light and (2) form an impact crater (Ref. 1). It was believed that if either or both of these reactions were of sufficient magnitude, they could be observed here on earth. Whether or not a lunar probe (or meteoroid) can cause an impact flash of this magnitude will be estimated on the basis of the experimental results to be reported in this paper. An indication that impact flashes of this magnitude are obtained is given by a recent Russian paper (Ref. 2) which concluded that the impact of the Second Cosmic Rocket on the moon caused an impact flash that was observed by at least a dozen observers in various parts of the world.

In contrast to the Russian observations, astronomers have attempted for years to observe the impact of meteors on the moon (Refs. 3-6) without drawing any significant conclusions. Recently, however, observations of meteor impacts on the lunar surface have been reported (Ref. 7), and from these an estimate was made that marble-sized meteors striking at 54,000 mph (78,000 ft/sec) can be seen with a 12.5-inch-lens telescope at 600 magnification. This estimate

of meteor size and velocity will be compared with the results of the laboratory impact studies later in this paper.

Experimental researchers have also attempted to look at the phenomena of impact flash (Refs. 8, 9) and cratering in rocks (Refs. 10, 11), but under conditions which may be inapplicable to the investigation of lunar impact flash. Consequently, the GM Defense Research Laboratories, General Motors Corporation, undertook a program to determine some specific features of a lunar impact, including reaction to a lunar probe of relatively high velocity. Results of this program may make it possible to discover the composition of lunar surface material.

It will be of major importance to the Ranger Program to obtain clear evidence that the probe actually contacted the surface of the moon, to ascertain where the impact occurred, and to gain some knowledge of the composition of the moon's surface from the impact. Whether or not the impact of the probe will provide this information depends upon the peak intensity of the flash, the duration of the flash, and the spectral distribution of light in the flash. If these aspects of the phenomena are known, it will be possible to design instruments for recording the flash and to estimate the feasibility of using data from these instruments to provide a record of the conditions of the impact. It may also be possible, through the proper choice of materials from which the probe is made, to augment the chances of success in the test by increasing the luminosity of the flash. Therefore, the experiments were designed to permit observations and to describe quantitatively the phenomena of impact flash, peak luminosity, time duration, and the spectrum of light emitted.

The first environmental condition to be considered is the effect of the gas at the target surface. Since most experiments on high-speed impact have been made with gas at appreciable pressure – that is, many orders of magnitude greater than pressure near the lunar surface – it is essential to learn the effect of pressure on impact flash if results of laboratory experiments to predict the phenomena of impact flash on the moon are to be used. Early work at the University of Utah (Ref. 9) indicated that the gas surrounding the target played an important part in producing the impact flash. This conclusion was based on the observation, in metal-to-metal impact, of a line spectrum attributed to the reaction of the surrounding gas with a high-velocity spray thrown out of the crater during the crater's formation. Therefore, it may be concluded that an impact on an atmosphere-free moon will not cause a flash. These conclusions will be shown to be not applicable to the case in point, since both the early experiments by the NASA-Ames Laboratories (Ref. 1) and the tests to be described show that impact flash is obtained under reduced ambient gas pressures.

The second condition to be considered is that of the materials comprising the lunar surface upon which the impact will occur. This composition is in fact unknown, and investigators are confused by contradictions found in hundreds of papers published on the subject. Suffice to say, the majority of references agree that the rough and cratered lunar surface was caused by the impact of meteors occurring over the eons following the solidification of the entire lunar mass. According to currently accepted views, the moon's surface is a rocky rubble covered with a thin layer of dust (Ref. 12), its composition and character undoubtedly varying from place to place and including, perhaps,steep slopes of bare rock in the mountainous regions.

To simulate the varied character of the lunar surface in the laboratory, it is desirable to make targets of a number of materials ranging from hard rock to extremely small-grain, well-packed particles. The target materials to be tested are as follows: (1) hard rock having a density of approximately 3 gms/cc; (2) large rocks loosely dispersed in a matrix of fine sand; (3) well-settled rock particles having a size distribution of from 0.1 to 1.0 millimeters; (4) well-settled sand having a particle size distribution from 10 to 1,000 microns; and (5) layers of sand of varying particle sizes piled on top of hard rock.

The other environmental conditions to be considered are those relating to the lunar probe. The probe will have a given size, be made of a certain material, and strike at a specified velocity. It should be noted that the Ranger vehicles will impact the moon at a velocity close to 10,000 ft/sec – a speed easily attainable in the laboratory. However, a projectile velocity range of 5,000 to 25,000 ft/sec will be used to evaluate velocity scaling effects. The vehicles will be made of metals and plastics; these also can be duplicated in the laboratory. On the other hand, the vehicle will weigh more than 700 pounds, and projectiles of this weight are beyond the capability of the tests in this program. Accordingly, part of the investigation was concerned with projectiles of different sizes to determine scaling laws for extrapolating the results of the laboratory to the conditions of full-scale flight.

SECTION II

RANGE AND MONITORING INSTRUMENTATION

The tests were conducted in the GM Defense Research Laboratories Ballistics Ranges 'A' and 'C'. Ballistics Range 'A' is fully described in GM DRL Report No. ER62-201A and Ref. 13. The basic facility consists of a gun, a 20-foot flight range, and an impact chamber (Fig. 1). The projectile is launched into the horizontal flight range by either of two guns (Figs. 2, 3): a 0.22-inch accelerated-reservoir light-gas gun (AR-LGG); or a 0.22-inch SuperSwift smoothbore rifle. The choice of guns depends upon the desired projectile mass and velocity. The 0.22-inch AR-LGG may be fired horizontally at velocities up to 32,800 ft/sec, while the SuperSwift rifle is used when the velocity requirement does not exceed 10,000 ft/sec (Fig. 4). The SuperSwift rifle may also be fired vertically using the facilities of Ballistics Range 'C' (vertical). Figure 5 shows a shortened version of this range with the 0.22-inch SuperSwift rifle installed. This vertical firing capability is especially useful when nonsolid targets such as sand or crushed stone are used. In these cases, no alien binders are required to maintain the shape of the target.

Both ballistics ranges are equipped to monitor projectile, target, and impact flash parameters. Hence, the following discussion of data-collection techniques is applicable to both.

During the course of flight, the model's position and time of flight are recorded at each of three spark shadowgraph stations in an

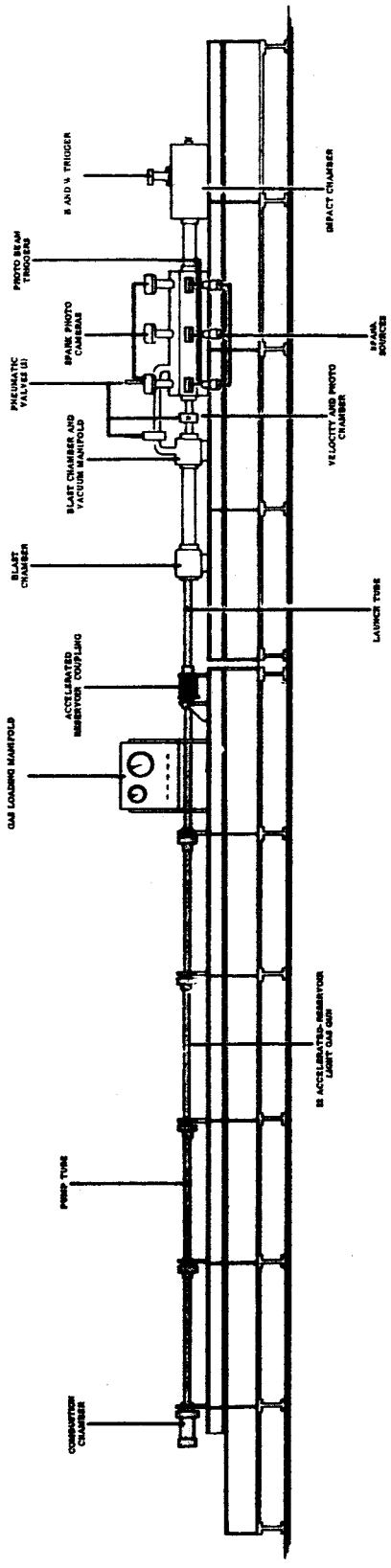

Fig. 1 Schematic of Ballistics Range "A"

Fig. 2 The 0.22-Caliber Accelerated-Reservoir Light-Gas Gun – Ballistics Range "A"

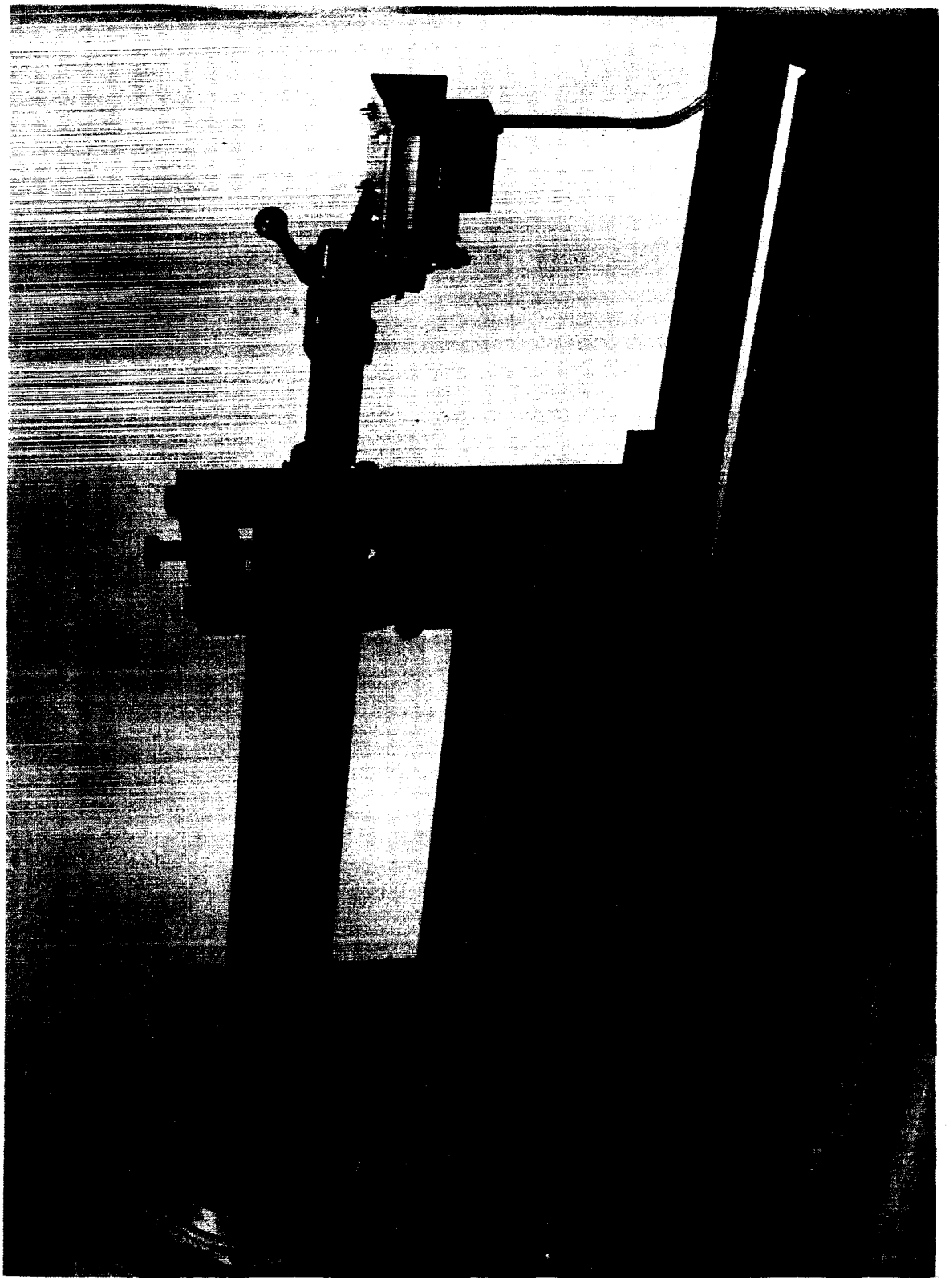

Fig. 3 The 0.22-Inch SuperSwift Smoothbore Rifle – Ballistics Range "A"

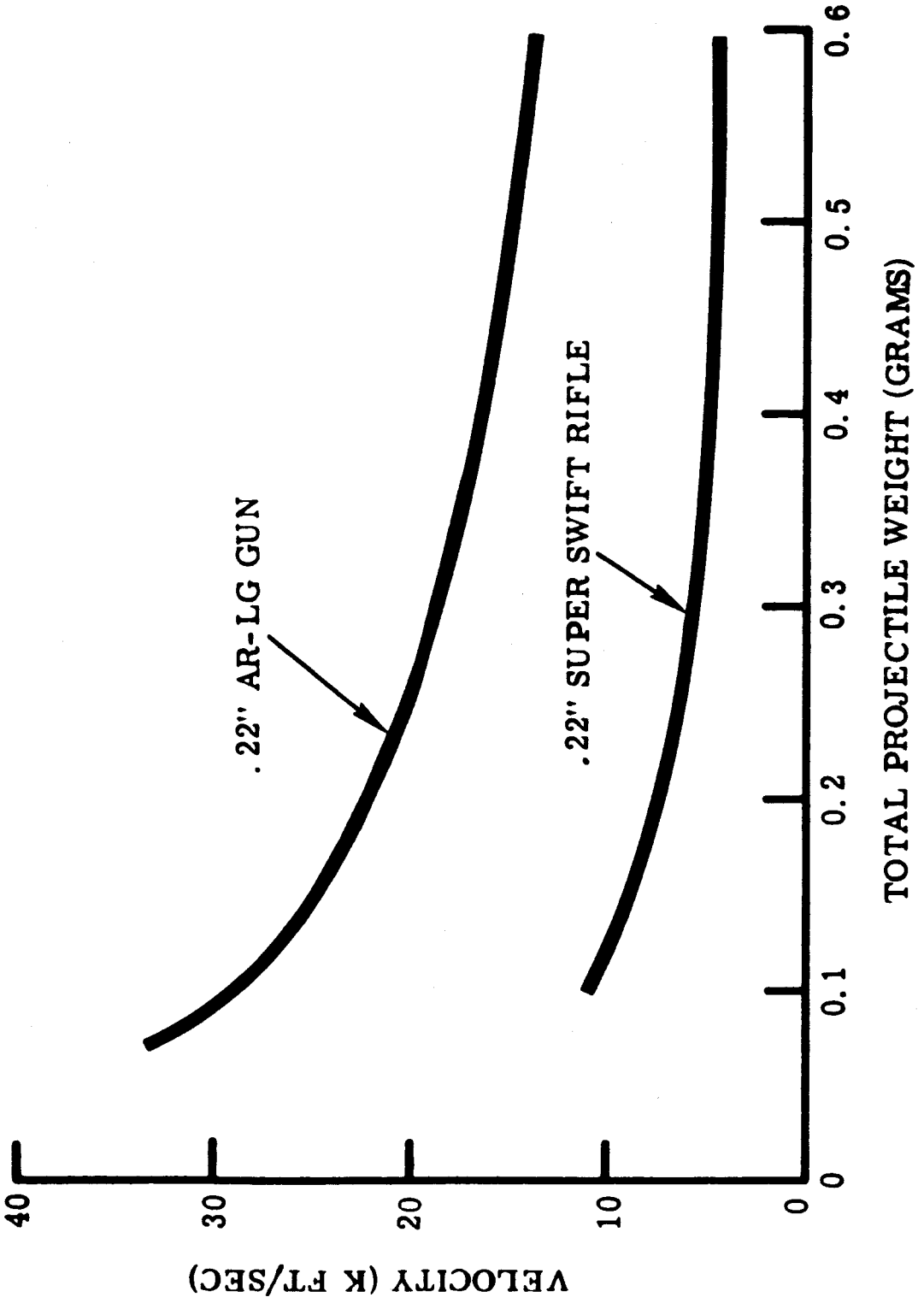

Fig. 4 Summary of Launcher Performance

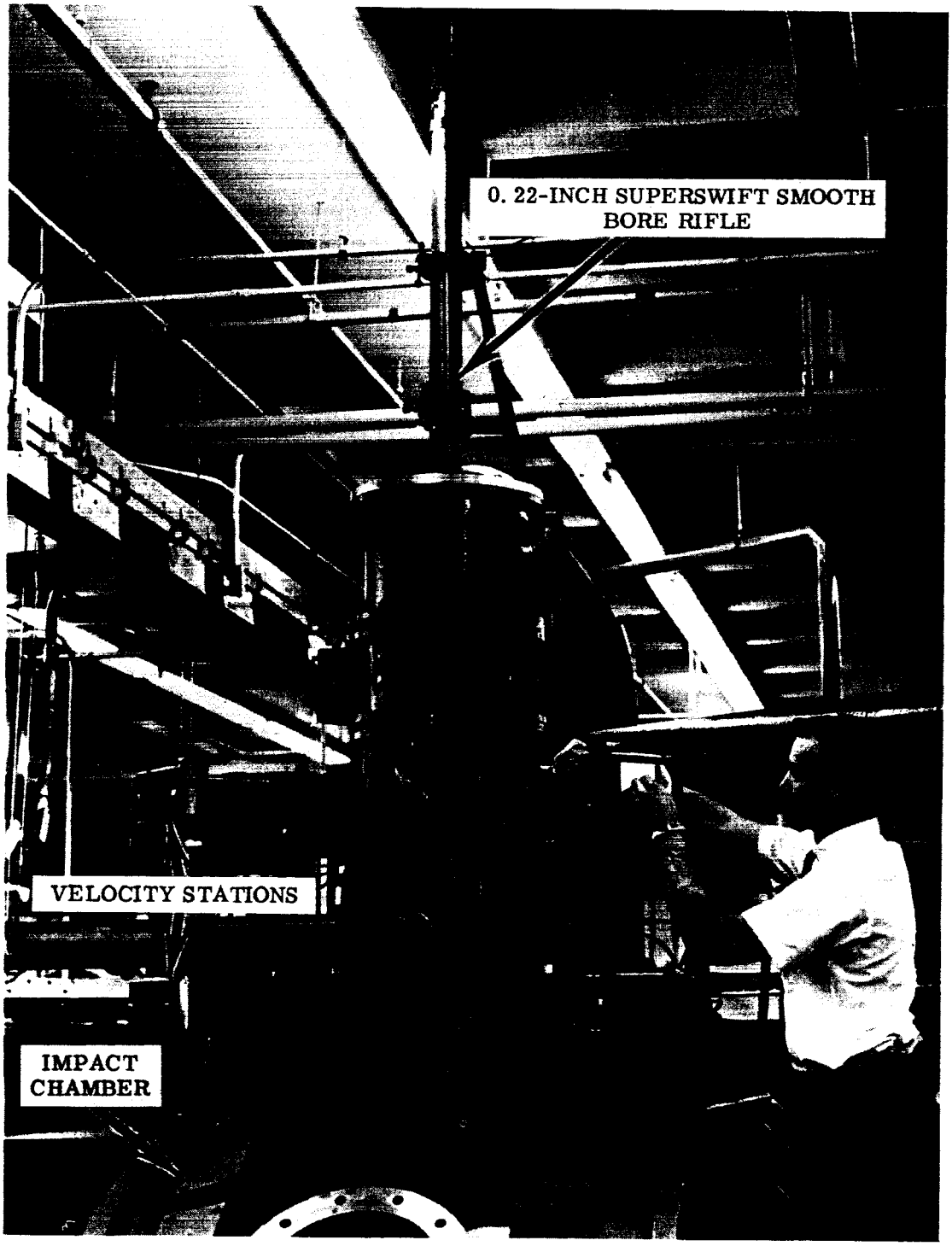

Fig. 5 Ballistics Range "C" (vertical)

instrumented velocity chamber (Fig. 6). Figure 7 is a schematic of the instrumentation associated with each station. When the model interrrupts the photobeam, electronic counters are started and a short-duration spark exposes a film plate. Figure 8 is a shadowgraph which shows a spherical model separated from its sabot at a velocity of 21,000 ft/sec. These measurements of time and distance of the projectile between stations serve to determine velocity along the trajectory and, in particular, at the target. The accuracy of the impact velocity determined in this manner is within one percent. The spark shadowgraph pictures obtained for the velocity computations show model condition and orientation prior to impact. This information, together with projectile weight taken prior to the launch, define mass and velocity at impact.

The model flight terminates in a specially constructed impact chamber (Figs. 5, 6) which has numerous viewing ports. The rear wall of the chamber, a full-size door, allows easy insertion and removal of the targets. The targets are held by a mount attached to the floor of the chamber. The impact and velocity chambers are vacuum-sealed and can be evacuated to pressures of less than one micron of mercury. Air or any desired gas or gas mixture can be introduced into the chamber as a test medium. An alphraton vacuum gauge and mercury manometers provide accurate and reliable pressure measurement.

Photographic and photoelectric equipment and open-shutter cameras with black-and-white or color film have been used to monitor the impact flash. Because initial records showed that radiation from the impact flash lay primarily in the visible and near infrared, quantitative optical monitoring devices were chosen for their response to these wavelengths. The three photomultiplier tubes used to record peak luminosity and

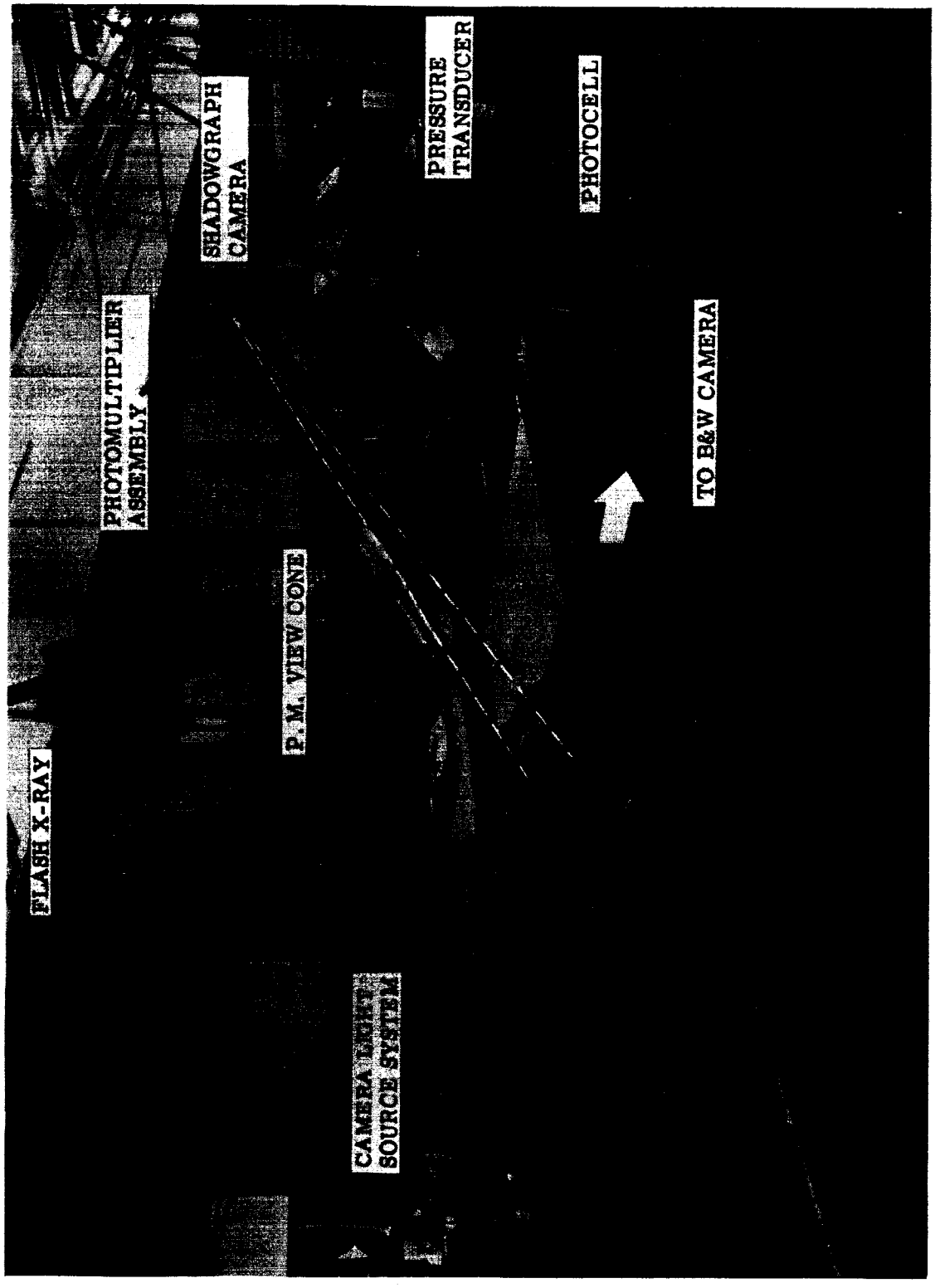

Fig. 6 Velocity and Impact Chambers – Ballistics Range "A"

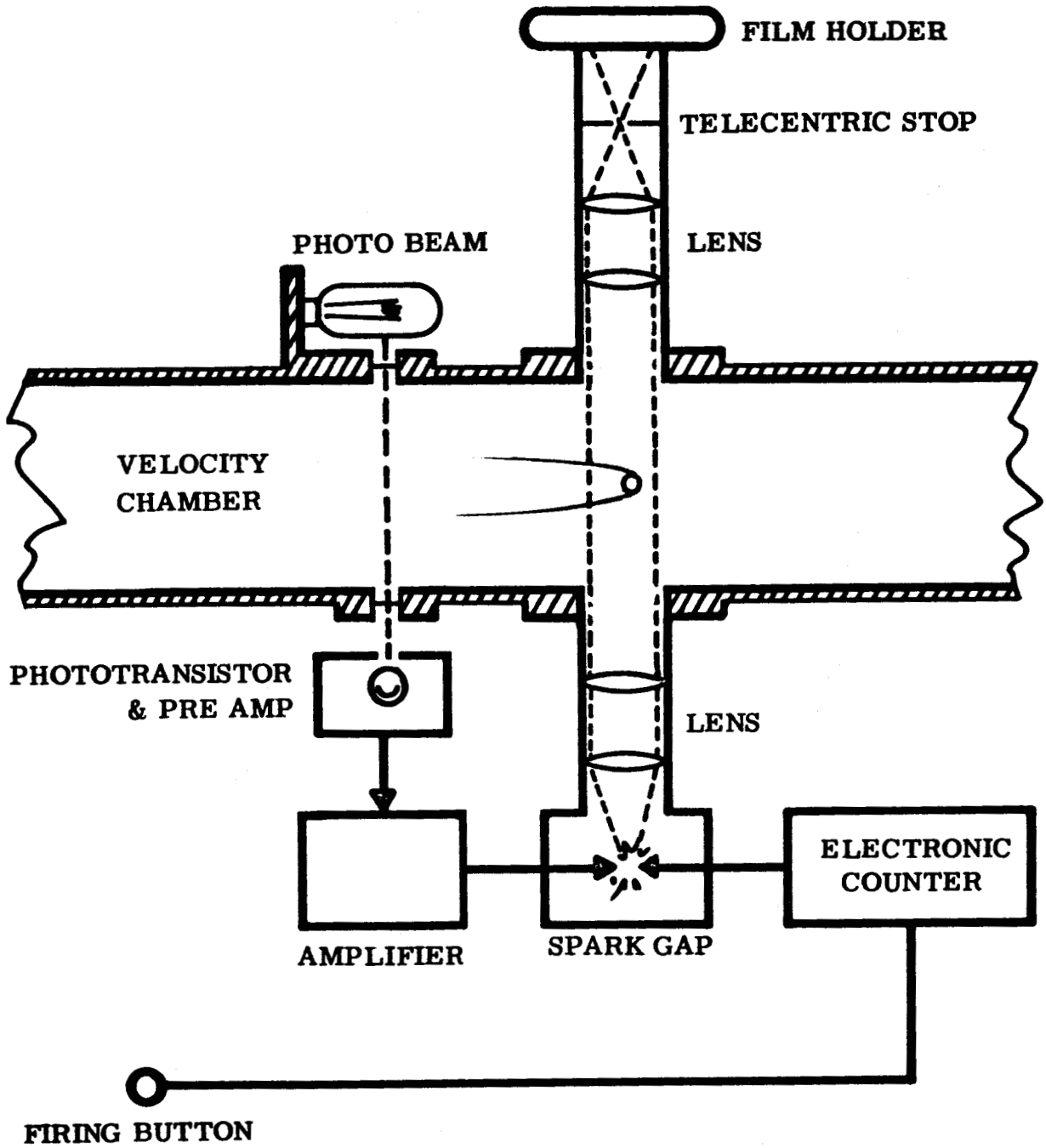

Fig. 7 Schematic of Ballistics Range Velocity Station

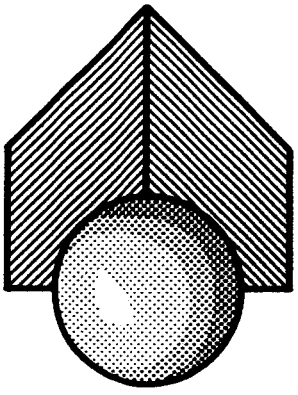

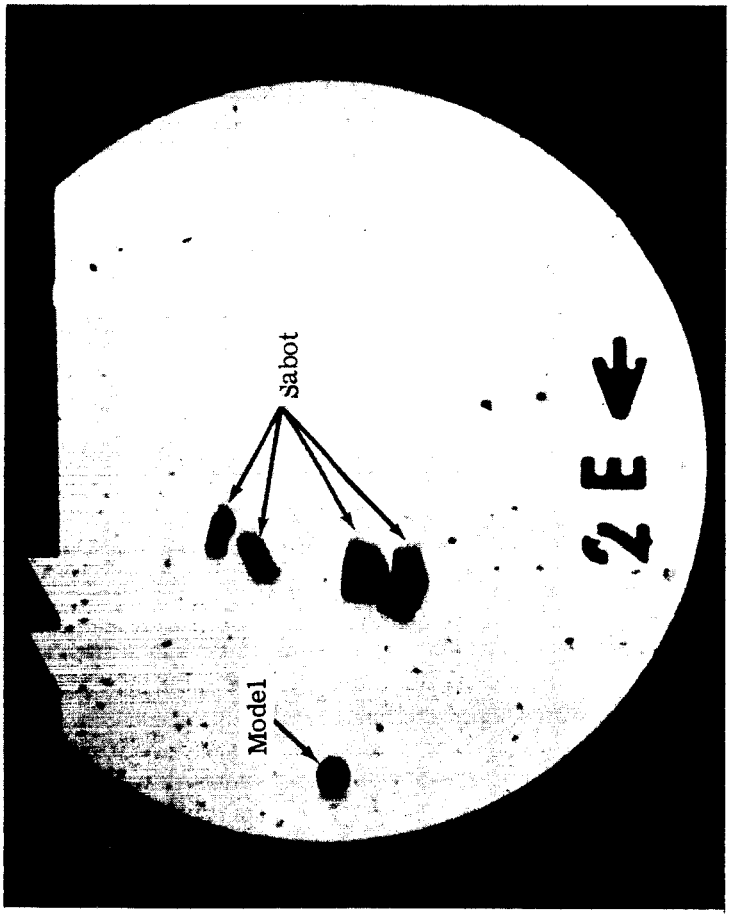

Fig. 8 Typical Shadowgraph Showing Separation of Model and Sabot

total time duration of emitted light were as follows: a PM tube (Dumont Type 6911) sensitive with filter to infrared radiation from 5,940 A to 10,000 A, and without filter to radiation from 4,500 A to 10,000 A; a PM tube (Dumont Type 6292) sensitive to the visible spectrum from 3,500 A to 5,500 A; and a PM tube (Dumont 7664) sensitive to the region from 1,800 A to 5,500 A. The PM tubes were calibrated to measure radiance in watts per unit-solid-angle as a function of both impact velocity and ambient gas pressure in the impact chamber.

To study the emitted spectra from a point 20° off normal, a spectrograph was built and placed on the impact chamber. The optical train and installation of this spectrograph are shown in Fig. 9. The system had a typically nonlinear dispersion of from 100 A/mm to 300 A/mm (total dispersion 30 mm) and a resolving power of less than 20A. The spectrograph was calibrated with a point-source mercury lamp which also served to locate the position of the impact on the vertical axis of the film.

In addition to the quantitative analysis of the light emitted during the impact flash, the phenomena were observed with the Beckman & Whitley Model 192 framing camera. This camera, capable of framing rates as high as 1.4 million frames per second, can be used to record precisely the (1) incoming projectile velocity, (2) the phenomena of impact flash, and (3) the motion, velocity, and approximate quantity of minute particles being ejected from the crater. This camera also makes it possible to observe, in a plane across the surface of the target, the growth of the crater in time.

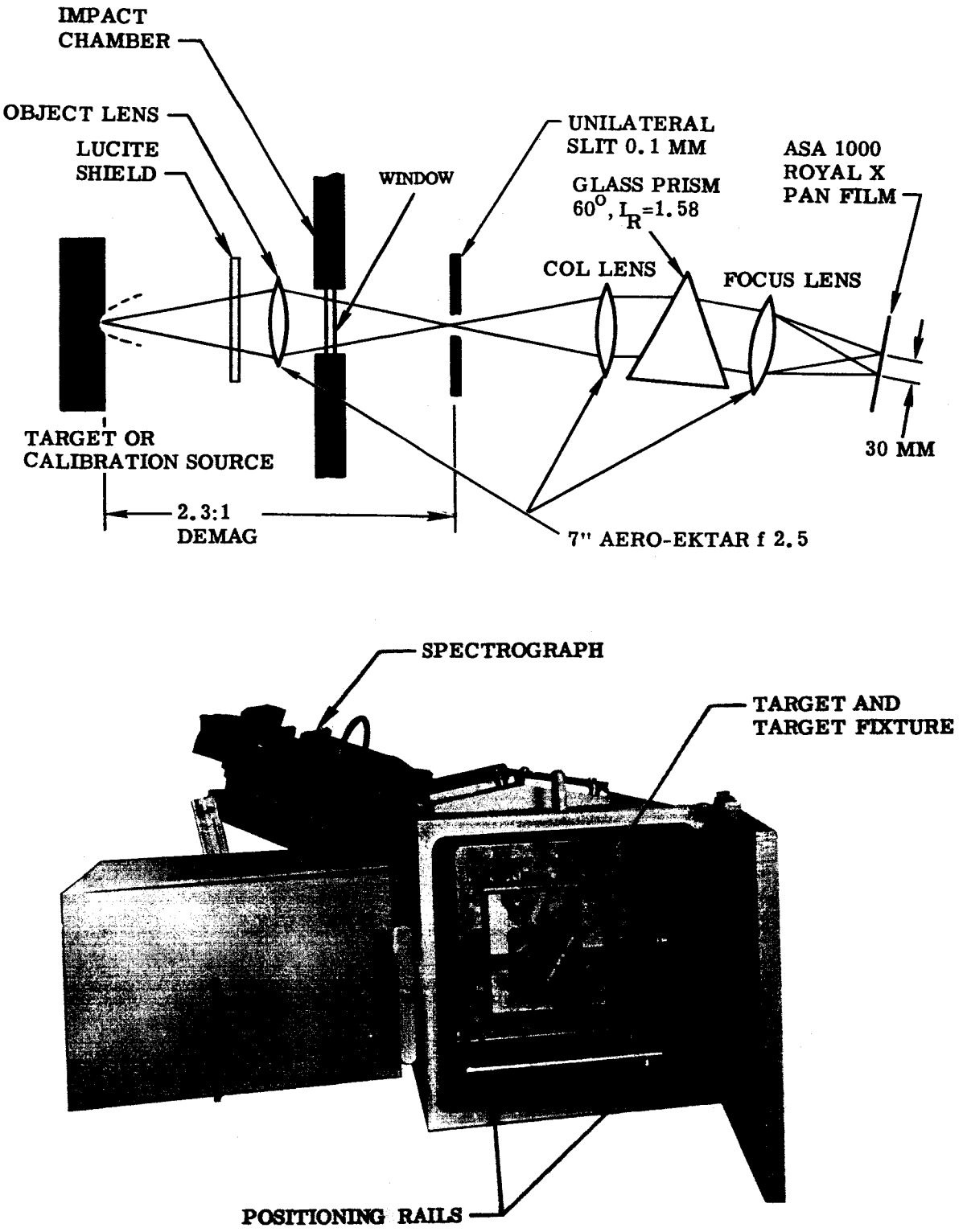

Fig. 9 Spectrograph Optical Train and Installation

SECTION III
RESULTS AND ANALYSIS

The experiments have been conducted with projectile materials of nylon, zelux, high-density linear polyethylene, pyrex, aluminum, steel, magnesium, brass (hollow and solid), and silver (hollow and solid). These projectiles ranged in diameter from 1/32 inch to 0.22 inch, and were launched at velocities ranging from 5,800 to 24,000 ft/sec.

The majority of the tests were conducted using sand, granite, or aluminum targets. Two types of sand were used. The first, commercially known as "Nevada 135", was a fine-grade silicon sorted through a 100-mesh screen and retained on a 200-mesh screen. Because of the Ballistics Range 'A' requirement to fire all shots horizontally, this sand was mixed with one percent linseed oil and two percent water (by weight) and cured at 400°F for approximately four hours in an air atmosphere. The second type was a commercial, washed, construction-grade sand with particle sizes ranging up to 1 mm. When this sand was used as targets for Ballistics Range 'C' (vertical) no binder was required. The granite, commercially known as "Georgia Grey", was polished on one side only. The aluminum was commercially known as 1100 F and was cleaned prior to firing.

A portion of the tests were conducted using basalt, peroditite, and gabbro targets. The basalt was used as targets in the following configurations:

1. Semi-infinite blocks – polished
2. Crushed – particle size from 0.1 mm to 1 mm
3. Crushed – particle size from 10 microns to 100 microns
4. Semi-infinite blocks – weathered, as received.

Chemical and semi-quantitative spectrographic analyses of these samples were performed by the Hornkohl Laboratories, Inc., of Bakersfield, Calif. The results are tabulated in Tables I and II. The peroditite and gabbro targets were used in a weathered, "as received" condition.

Table I

BASALT

CHEMICAL ANALYSIS

Constituents		Sample No. 140928 1 (small)	140929 2 (medium)	140930 3 (large)
Silica	(SiO_2)	63.06%	61.84%	61.08%
Alumina	(Al_2O_3)	12.90%	15.21%	14.66%
Iron Oxide	(Fe_2O_3)	5.42%	7.29%	8.87%
Calcium Oxide	(CaO)	5.38%	4.98%	4.72%
Titanium Oxide	(TiO_2)	3.49%	3.16%	2.92%
Magnesia	(MgO)	5.18%	3.04%	3.19%
Sodium Oxide	(Na_2O)	2.32%	2.43%	2.18%
Potassium Oxide	(K_2O)	1.62%	1.55%	1.60%

Table II

BASALT
SEMI-QUANTITATIVE SPECTROGRAPHIC ANALYSIS

	Sample No.		
	140928 1 (small)	140929 2 (medium)	140930 3 (large)
Major Constituents			
Silicon	Over 10%	Over 10%	Over 10%
Intermediate Constituents			
Aluminum	5 – 10%	5 – 10%	5 – 10%
Iron	5 – 10%	5 – 10%	5 – 10%
Calcium	5 – 10%	5 – 10%	5 – 10%
Magnesium	1 – 5%	1 – 5%	1 – 5%
Titanium	1 – 5%	1 – 5%	1 – 5%
Sodium	1 – 5%	1 – 5%	1 – 5%
Minor Constituents			
Potassium	0.5 – 1.0%	0.5 – 1.0%	0.5 – 1.0%
Phosphorus	0.05 – 0.1%	0.05 – 0.1%	0.05 – 0.1%
Manganese	0.01 – 0.05%	0.01 – 0.05%	0.01 – 0.05%
Boron	0.005 – 0.01%	0.005 – 0.01%	0.005 – 0.01%
Strontium	0.001 – 0.005%	0.001 – 0.005%	0.001 – 0.005%
Molybdenum, Cobalt, Vanadium, Copper, Nickel, Chromium	Trace	Trace	Trace

OBSERVATIONS OF THE IMPACT FLASH AND TARGET CRATER

Within the range of the experiments, an impact flash was observed under all test conditions. A typical impact flash observed by an open-shutter camera is shown in Fig. 9. A study of more than 600 records of impact flashes shows that the intense luminosity in the center of the impact is associated with both the projectile and the area of the target under the projectile, while the striated luminosity surrounding the point of impact is associated with the debris ejected from the crater. These conclusions are in agreement with the flash pictures obtained at the Ames Research Laboratories (Ref. 1). Open-shutter flash pictures (Refs. 1, 9) depict a dark spot surrounded by an intense impact flash in the center of the impact. The dark spot is believed to be the opaque copper projectile used in those tests. In the picture shown in Fig. 10, however, of a translucent (nylon) projectile, the dark spot does not appear. Typical craters formed in both sand and granite targets are shown in Fig. 11.

EFFECT OF AMBIENT GAS AND PRESSURE

Since the impact of a lunar probe will occur in the absence of any atmosphere, it was necessary to test the effect of various ambient gases and gas pressures on the magnitude of the impact flash. In the pilot experiments of Fig. 12, nylon spheres were fired into sand targets under various conditions of velocity and ambient air pressures. The ordinate in this figure is the peak luminosity of the flash, I_{np} (in watts per steradian), which is equal to the measured value normal to the target surface. The peak luminosity, I_{np}, is then plotted as a function of both impact velocity and ambient range pressure. In Fig. 12a, three selected impact velocities were chosen and the values of

SIDE

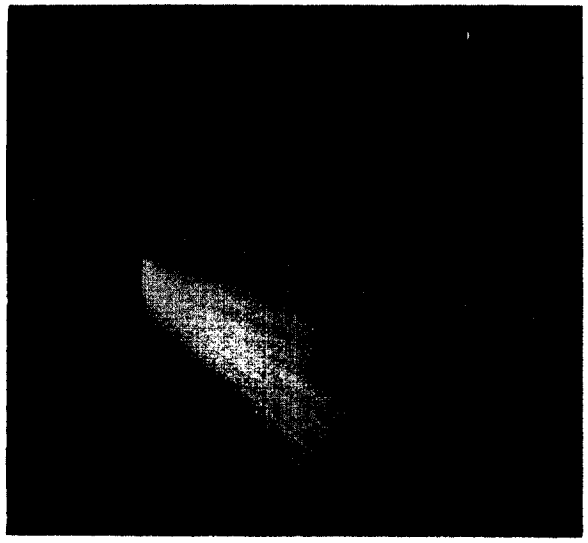

FRONT

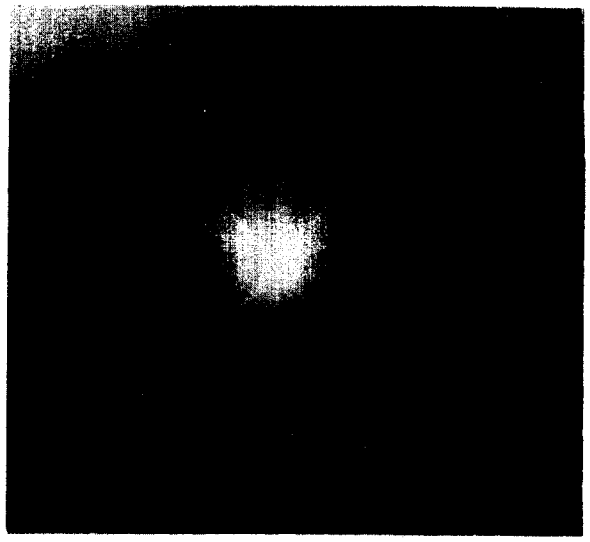

V= 10,360 ft/sec
P= 1mm Hg - AIR

Fig. 10 Typical Impact Flash in Sand (Nevada 135)

V= 8440 ft/sec
P= 1 mm Hg - AIR

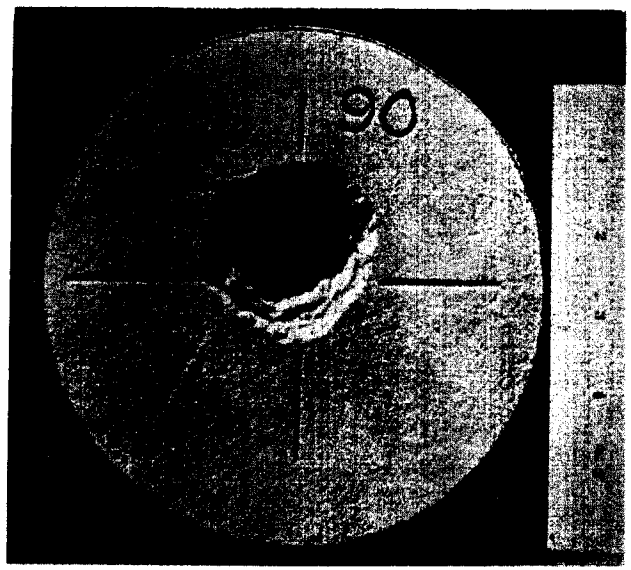

SAND TARGET
"Nevada 135"

V= 10,360 ft/sec
P. 76mm Hg - AIR

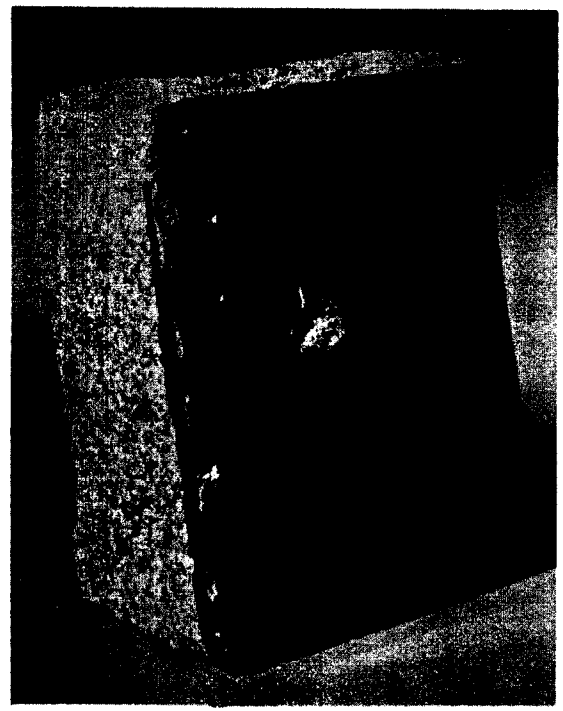

GRANITE TARGET
"Georgia Grey"

Fig. 11 Typical Impact Craters Formed in Sand and Rock

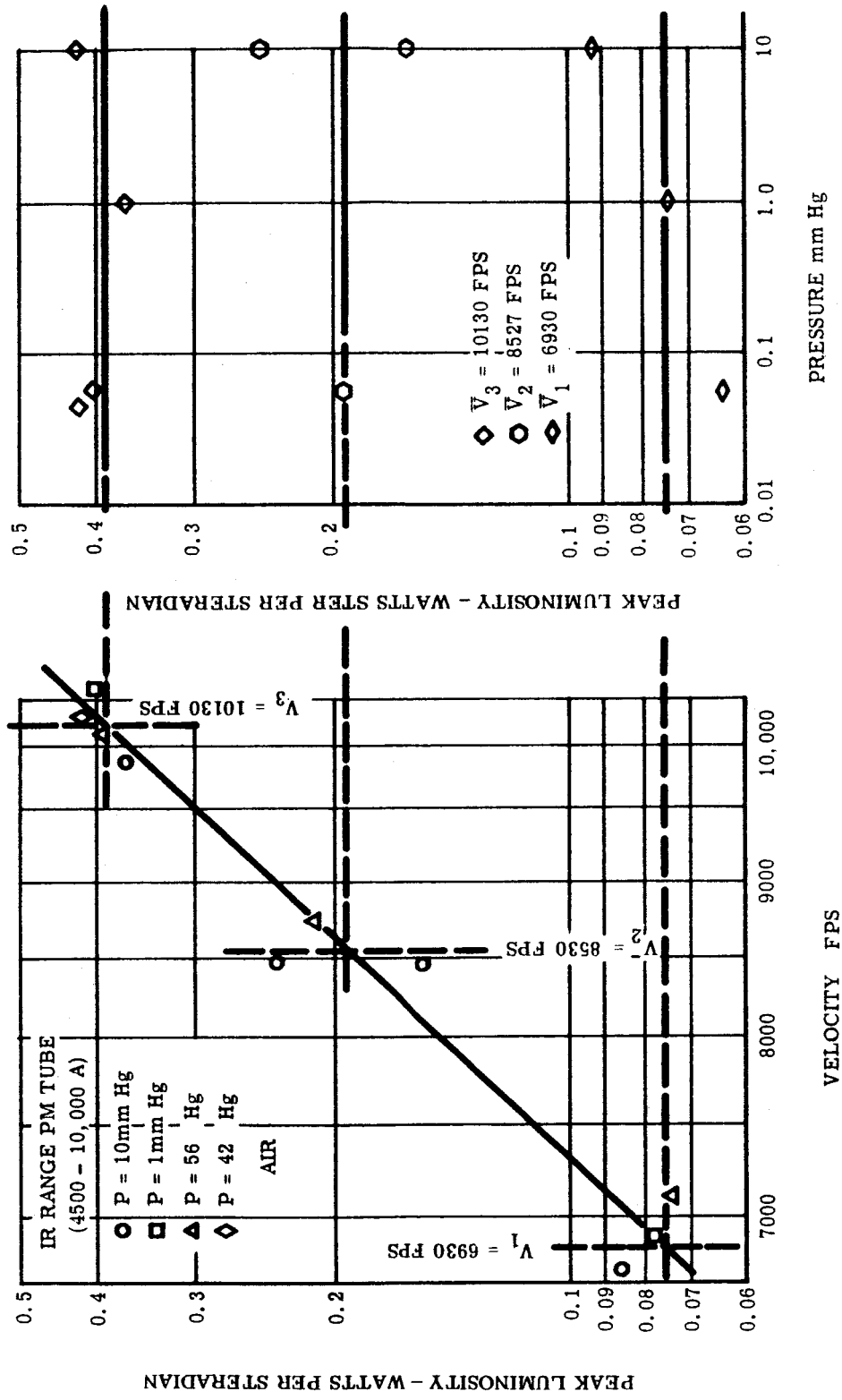

Fig. 12 Effects of Velocity and Pressure on Peak Luminosity from Impact of Nylon Spheres (0.22-In. Diam) on Sand Targets (Nevada 135)

I_{np} corrected to a best-fit slope of the data. These three velocities were then made the dependent variable and the data points replotted as a function of ambient pressure. One important result of the research program is demonstrated by Fig. 12b. At ambient pressures of 10 mm of Hg and down to 0.042 mm of Hg (nearly three orders of magnitude change in pressure), the magnitude of the peak luminosity of the impact flash did not vary significantly. Extrapolation of these data to lower pressures would indicate that the flash is independent of the surrounding pressure.

To further demonstrate this important conclusion, the tests were extended to include a test of the magnitude of the impact flash over a wider range of pressures in air and to test the impact flash in an inert atmosphere. To do this, nylon projectiles were fired against both aluminum and sand targets at pressures ranging from one micron of Hg to one atmosphere in environments of both air and helium. The resulting data (Fig. 13) demonstrate that there is little measureable effect of the surrounding gas or the ambient gas pressure on the peak intensity of the impact flash. In fact, only in the case of aluminum targets at air pressures over 10 mm of Hg was any significant increase observed.

EFFECTS OF VARIED PROJECTILE PARAMETERS AND TARGET MATERIAL

In order to determine the relationship of the impact flash to the many possible projectile parameters, experiments were conducted with projectiles of varied size, material, and velocity. The targets used in these tests consisted of either sand, granite, or aluminum. Some of the results of these tests have already been observed in Fig. 12a,

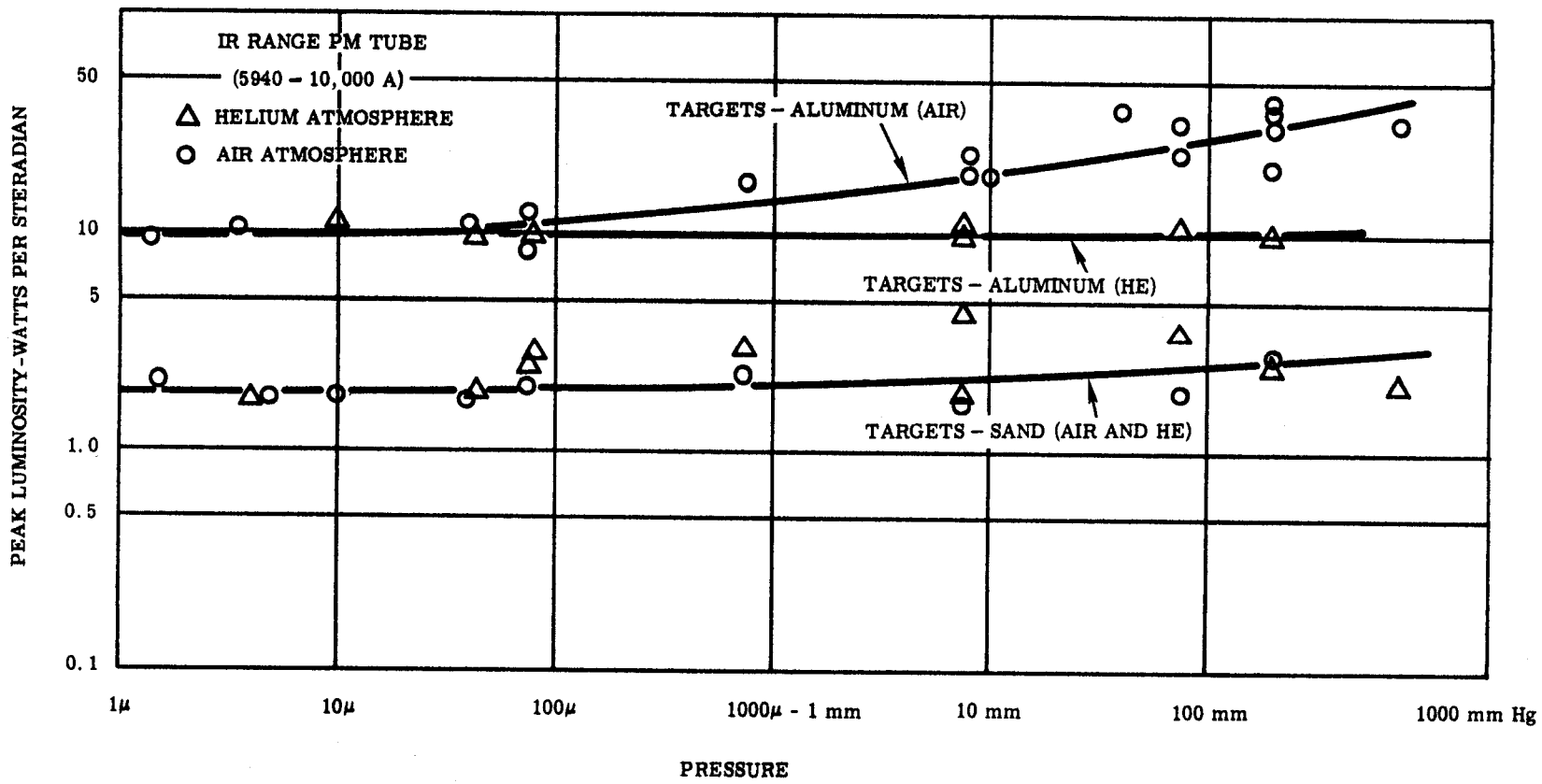

Fig. 13 Reduced Data – Variation of Peak Luminosity with Pressure for Nylon Spheres (0.22-In. Diam) Impacting Sand and Aluminum at 8,000 fps in Air and Helium

which shows that the intensity of impact flash increases with projectile velocity. Within the scope of the data obtained thus far, the intensity appears to increase as some power of the impact velocity (v^n).

With nylon projectiles against sand targets, the data of Fig. 12b show that I_{np} varies approximately as $v^{4.0}$. This relationship of I_{np} to impact velocity is further tested by the data shown in Figs. 14-17a. Using aluminum and glass projectiles to impact sand (Fig. 14) and aluminum projectiles against granite (Fig. 15), I_{np} can be seen to to vary as $v^{3.88}$ and $v^{4.95}$, respectively. For nylon projectiles vs aluminum targets (Fig. 16), I_{np} is seen to vary as the 3.5 power of velocity. In Fig. 17a, the data obtained from steel projectiles against sand targets indicate that I_{np} varies as $v^{8.30}$. Although the exact power relationships cannot yet be determined, it is anticipated that the exponent of velocity will lie between 3 and 9 for a variety of projectile sizes and materials against either sand, rock, or aluminum targets.

In addition to the velocity scaling effects, a third important conclusion is demonstrated in Figs. 17a and 17b. Values of I_{np} were taken from the plot for the case of four sizes of steel projectiles impacting sand targets at a constant velocity of 8,000 ft/sec. These four values of I_{np} were replotted as a function of projectile diameter as shown in Fig. 17b. A method of least square fit was then applied to these data points, with the result that the best fit of the data showed I_{np} to vary as the square of the projectile diameter (D_p). This technique was also applied to the data for various sizes of brass, aluminum, magnesium, and glass projectiles fired into both sand and aluminum

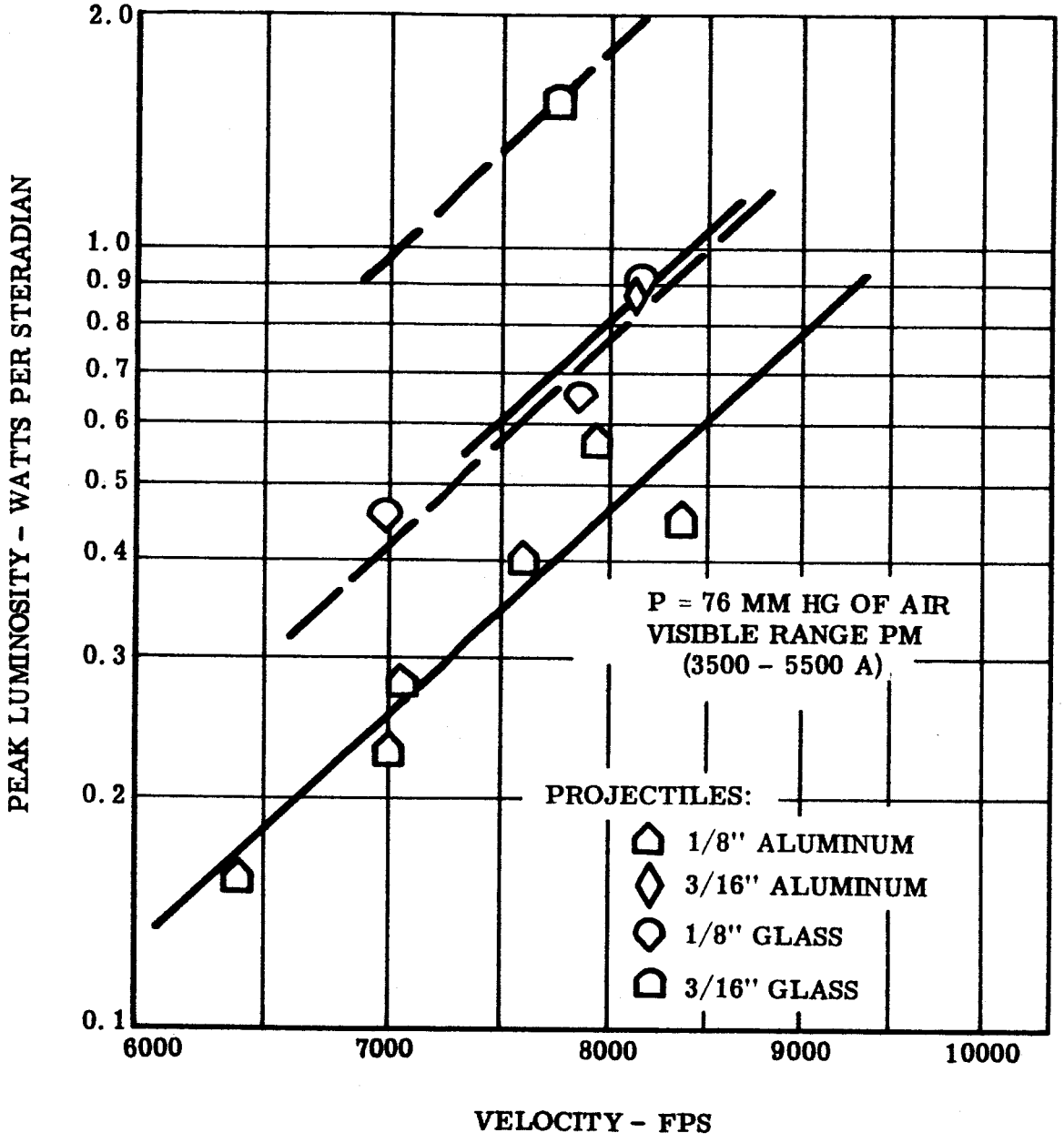

Fig. 14 Effect of Velocity on Peak Luminosity for Glass and Aluminum Spheres Impacting Sand Targets (Nevada 135)

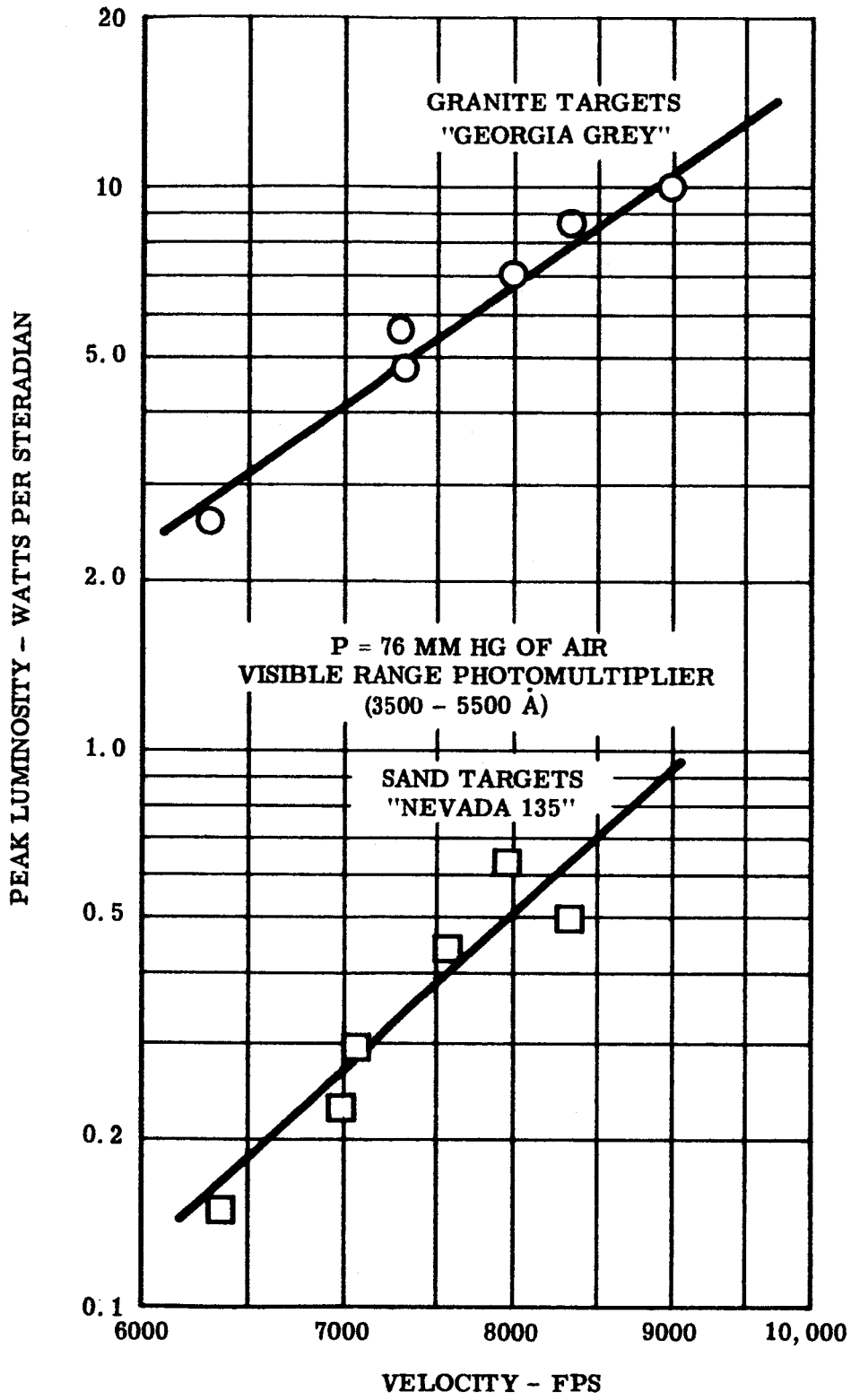

Fig. 15 Effect of Velocity on Peak Luminosity of Aluminum Spheres (1/8-In. Diam) Impacting Sand and Granite

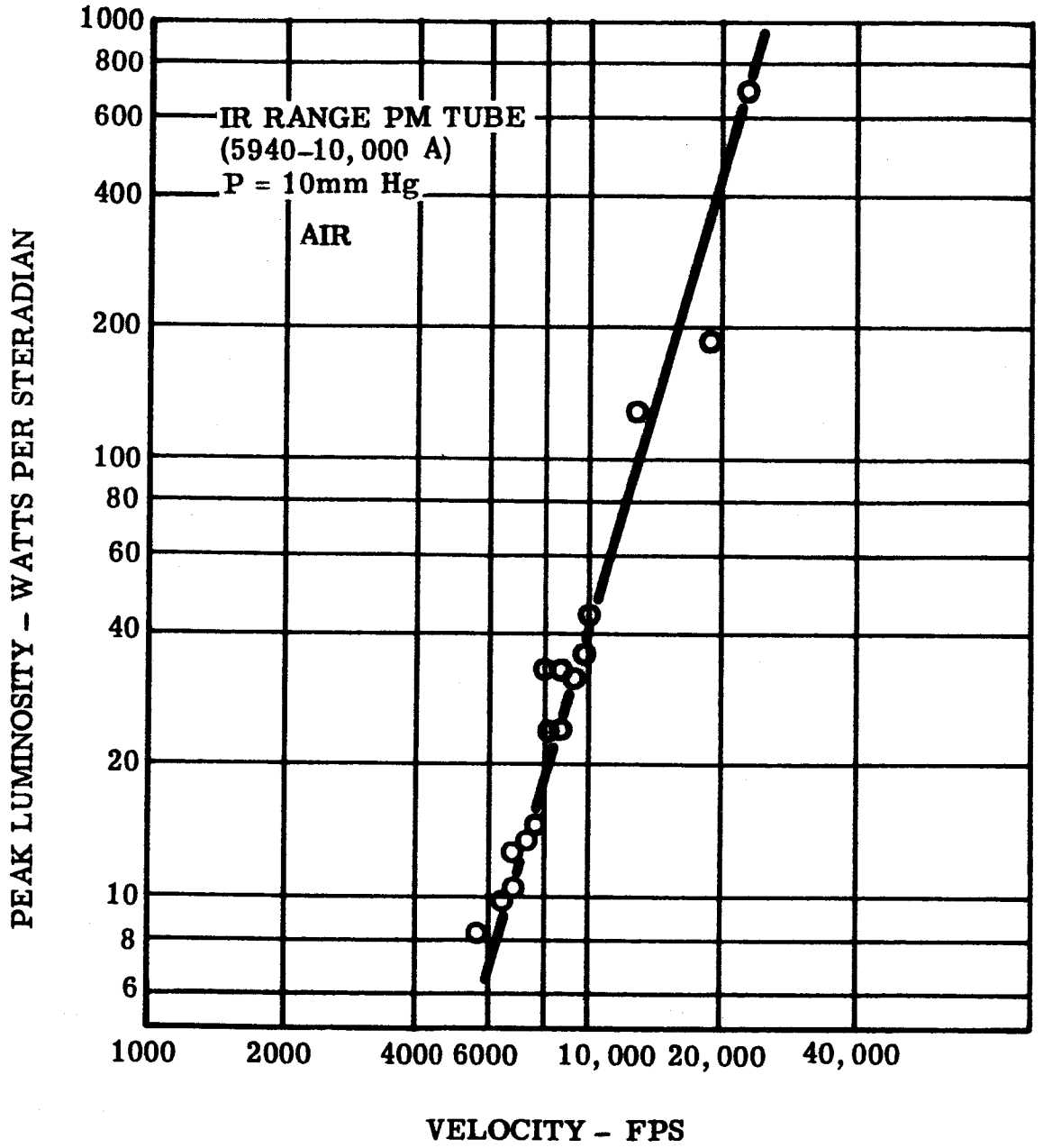

Fig. 16 Effect of Velocity on Peak Luminosity for Nylon Spheres (0.22-In. Diam) Impacting Aluminum Targets

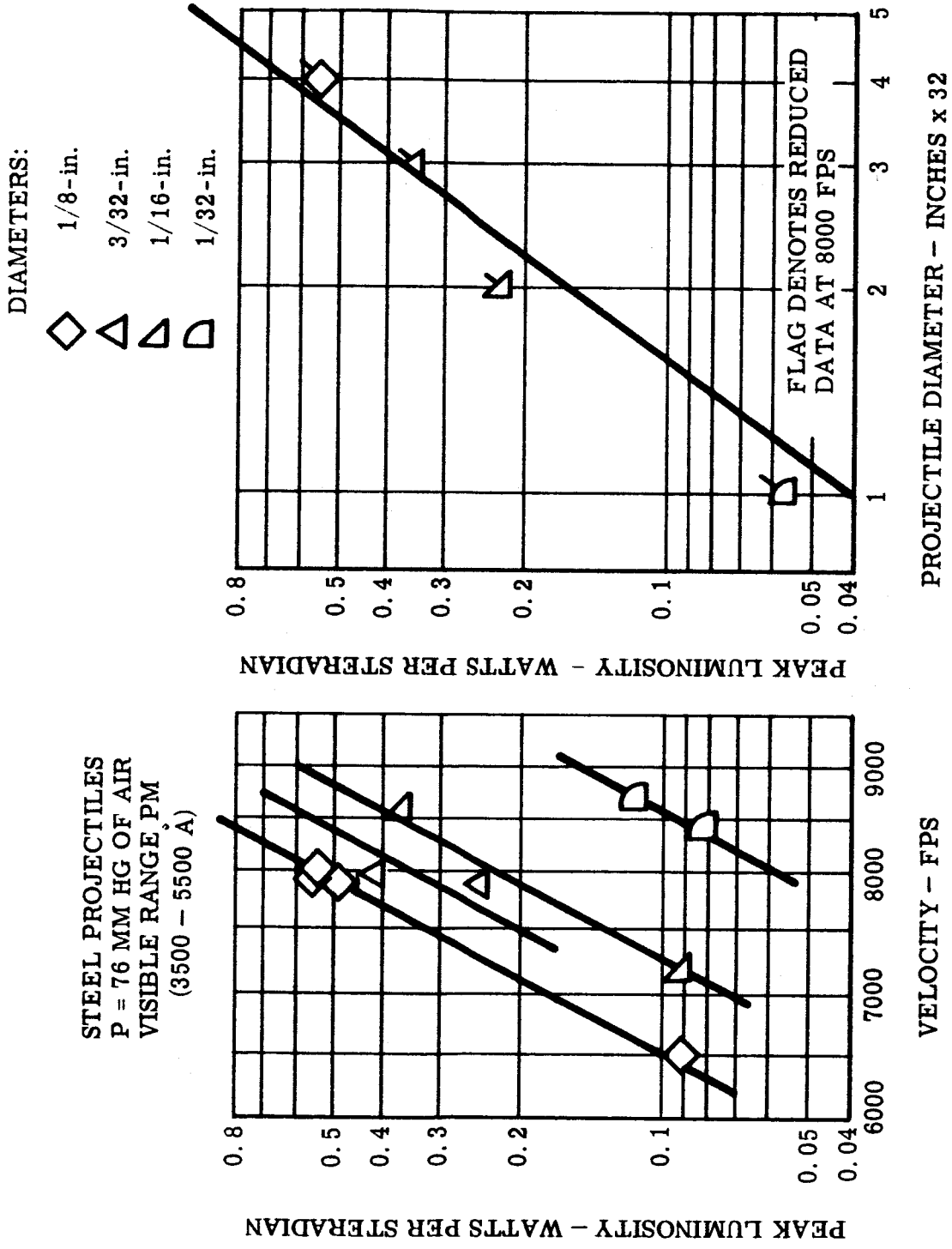

Fig. 17 Effects of Velocity and Projectile Diameter on Peak Luminosity for Steel Spheres of Various Sizes Impacting Sand Targets (Nevada 135)

targets (Fig. 18). I_{np} is shown to vary as D_p^2 for any combination of projectile and target and to be independent of the monitored frequency range, gas pressure, and the ambient gas.

It can be concluded (Fig. 18) that projectiles of the same surface area and material produce the same impact flash if fired under identical conditions and, from this, that the impact flash is a phenomenon associated with the surface area of the projectile rather than with its mass.

To further test the effect of projectile mass, projectiles of a variety of materials were fired under identical conditions. The result: all the metallic materials yielded the same impact flash (Fig. 19). To investigate further the effect of mass with metallic projectiles, hollow and solid brass spheres and hollow and solid silver spheres of the same diameter (1/8 in.) were fired at the same velocity against aluminum targets (Fig. 19). The surface areas of the two spheres were identical, of course, but the difference in mass between the two was 40 percent. Result: the peak luminosities of impact flashes were identical, and time durations of the two flashes were almost equal. These data support the data of Fig. 18, in which it was established that the intensity of the flash is a function of the area of the impacting projectile and not directly dependent upon momentum or kinetic energy. As an exception to this result, the data for nonmetallic projectiles (pyrex, nylon, etc.) indicate flashes of lower intensity than the constant-intensity flash observed from the metallic projectiles. Thus, it is indicated that the flash is a function of the properties of the projectile material as well as of the presented area. It is believed at this time that the significant properties of a projectile

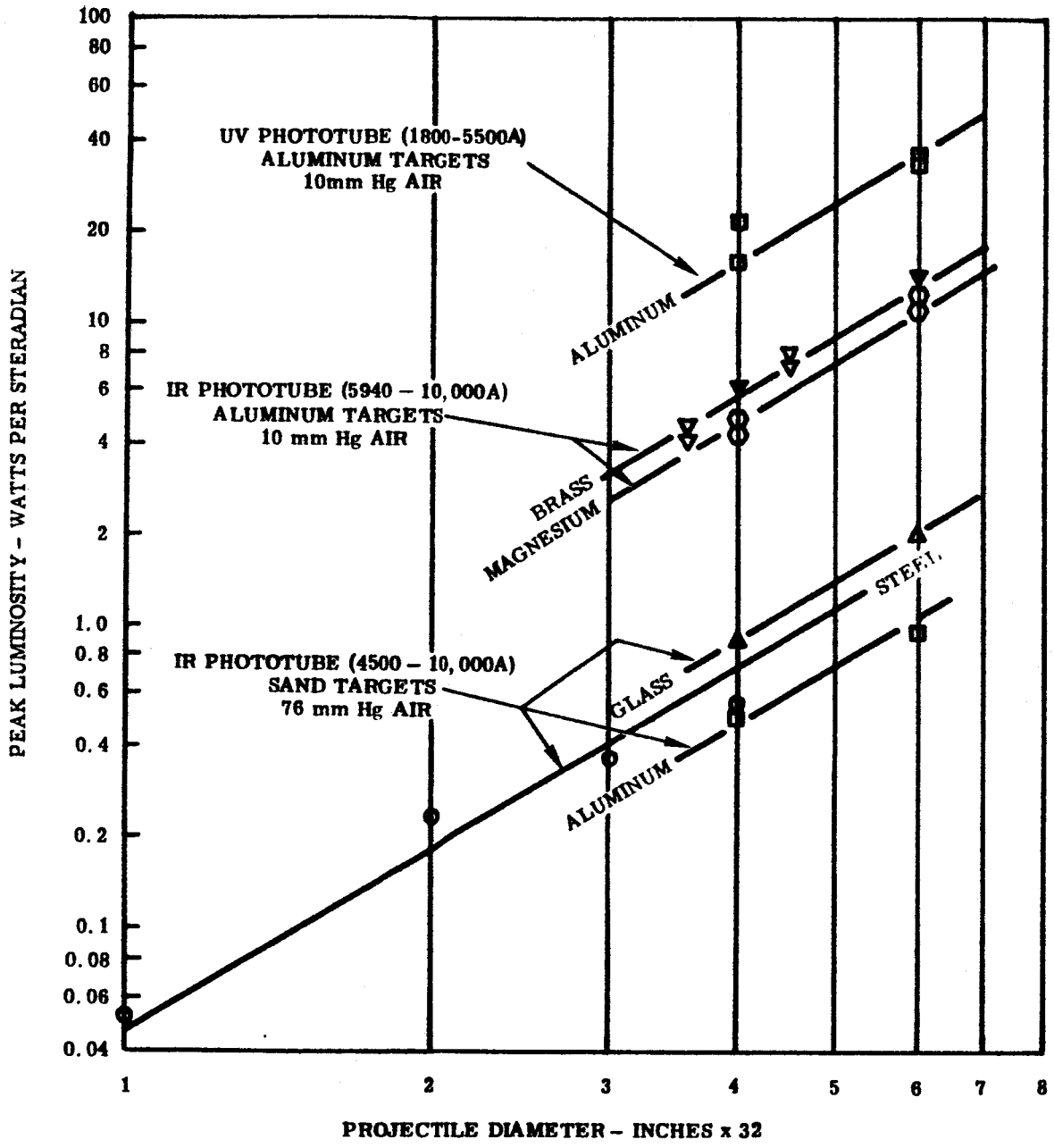

Fig. 18 Reduced Data – Variation of Peak Luminosity with Projectile Diameter (Velocity = 8,000 fps)

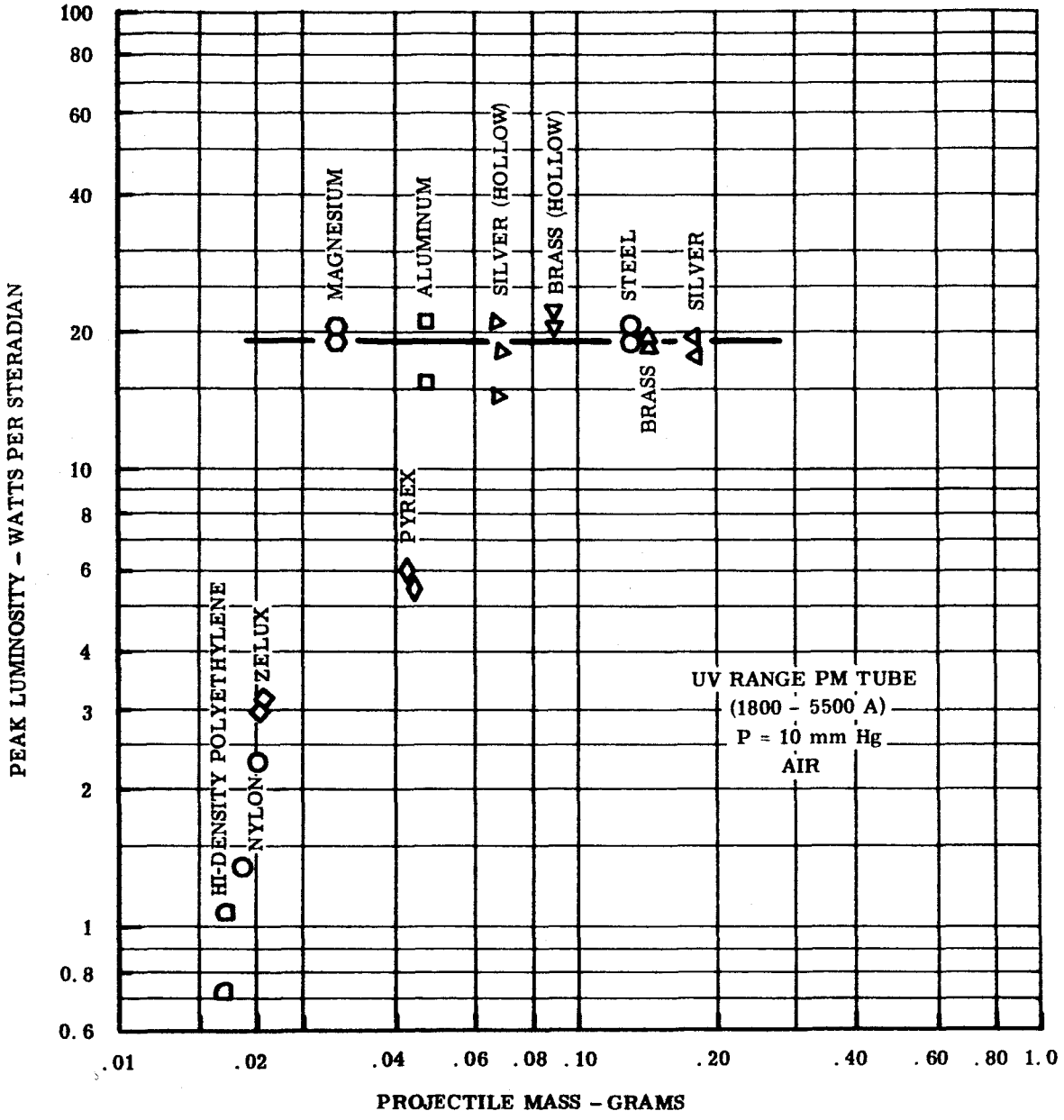

Fig. 19 Reduced Data – Variation of Peak Luminosity with Projectile Mass (Diameter = Constant = 1/8 Inch; Velocity = 8,000 fps; Target of 1100F Aluminum)

are those related to the hardness of the material, to the resistance of the material to dynamic deformation, and to the reactivity of the material under compressive loads.

Figure 15 shows that for a given projectile a change of target material produces a variation in impact flash; for example, the peak luminosity of the impact flash in granite is more than ten times that in sand. Also, over the range of velocities of interest here, the data are represented by a variation of peak luminosity, with approximately the fourth power of the velocity for granite and aluminum targets, and the fifth for sand targets.

All of the data presented so far has come from impact against simple targets, i.e., metal, polished granite, and sand. Since it has been postulated that the lunar surface consists of rock under varying layers of dust, tests of the occurrence and intensity of the impact flash with a more "realistic" target were needed. With nylon projectiles against various configurations of basalt, I_{np} varies approximately as $v^{5.16}$ (Fig. 20). The effects of a dust layer on semi-infinite basalt blocks is demonstrated in Table III.

A small number of rounds were also fired against semi-infinite gabbro and peroditite targets using nylon projectiles. However, no conclusions can be drawn from the data obtained because of scatter; this is attributed to the condition of the target surface – rough and weathered.

At this point, an empirical relationship to describe the results thus far can be written as:

$$I_{np} = CAv^{n} \quad \ldots\ldots\ldots\ldots\ldots\ldots \quad (1)$$

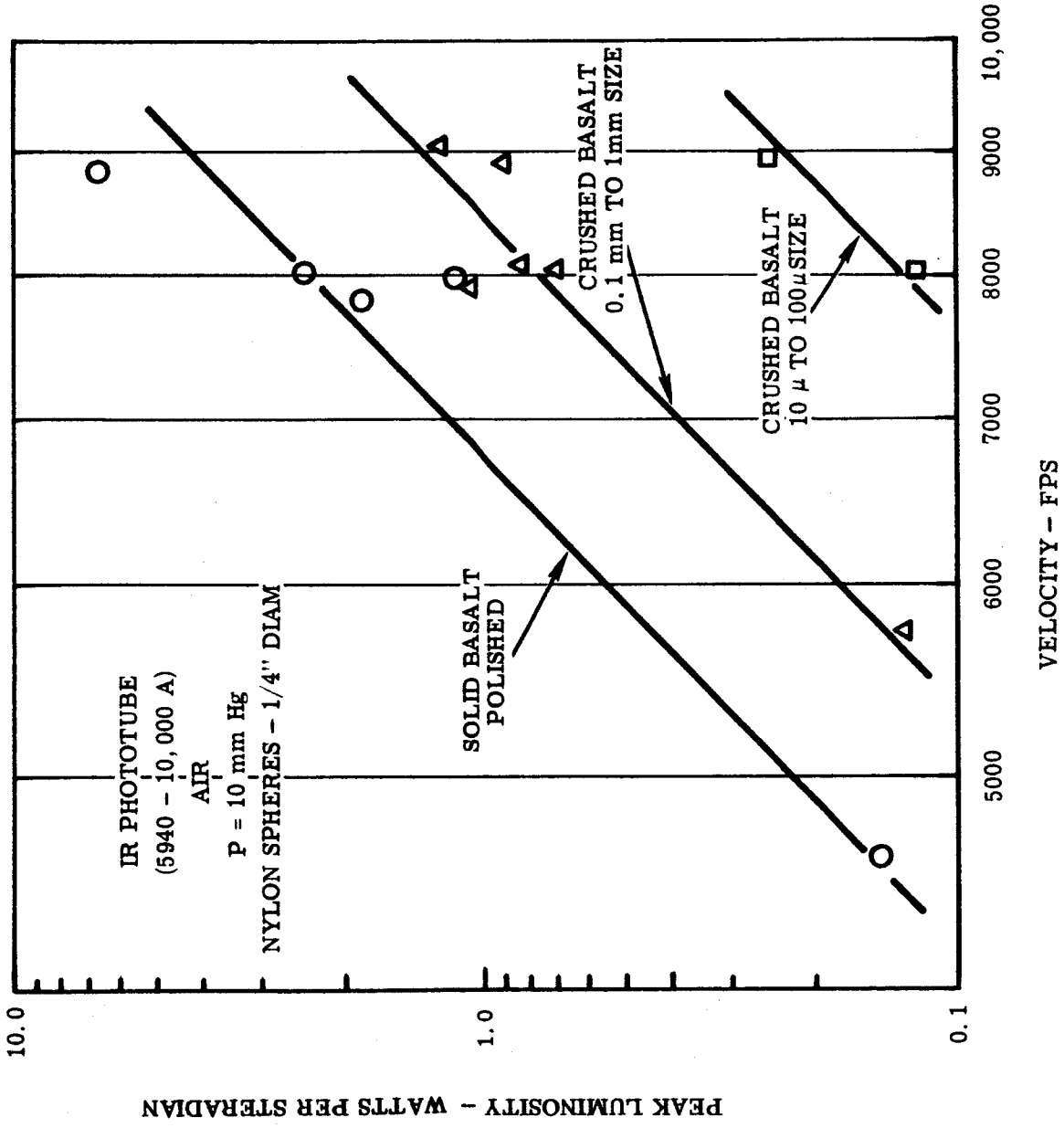

Fig. 20 Effect of Velocity on Peak Luminosity from Impact of Nylon Spheres (0.22-In. Diam) Impacting Various Basalt Targets

Table III

EFFECTS OF DUST LAYER ON SEMI-INFINITE BASALT BLOCKS

(IR Range PM Tube - 5940 – 10,000 A; P = 10 mm Hg Air; Data reduced to 8,000 fps)

TARGET CONFIGURATION	PEAK LUMINOSITY – WATTS PER STERADIAN	
	CRUSHED BASALT Particle Size – 0.1 mm to 1.0 mm	CRUSHED BASALT Particle Size – 10 μ to 100 μ
1. Semi-infinite basalt block	2.3 (Fig. 20)	2.3 (Fig. 20)
2. 1/16-in. layer of crushed basalt on semi-infinite basalt block.	0.785	0.98
3. 1/8-in. layer of crushed basalt on semi-infinite basalt block	0.778	0.30
4. Semi-infinite layer of crushed basalt	0.74 (Fig. 20)	0.125 (Fig. 20)

where I_{np} = peak luminosity (1800 – 10,000 A)

A = area of projectile on target surface

v = velocity of impacting projectile

n = velocity exponent $3 \leq v \leq 9$

C = a constant (a primary function of the target and a secondary function of the projectile)

Within the scope of the experiments conducted, measured values for the coefficient C are listed in Table IV for a variety of projectile-target combinations.

Table IV

VALUES OF TERMS IN EQUATION 1

Projectile	Target	C $\frac{\text{watts per sterad}}{\text{ft}^2\ (\text{fps})^n}$	n	Photomultiplier Range
Aluminum	Granite	0.059×10^{-9}	3.88	Visible (3500 – 5500A)
Aluminum	Sand (Nevada 135)	0.025×10^{-14}	4.96	Visible (3500 – 5500A)
Steel	Sand (Nevada 135)	0.030×10^{-27}	8.30	Visible (3500 – 5500A)
Glass	Sand (Nevada 135)	0.048×10^{-14}	4.96	Visible (3500 – 5500A)
Nylon	Sand (Nevada 135)	0.035×10^{-11}	4.02	Infrared (4500 – 10,000A)
Nylon	Crushed Basalt 0.1 mm to 1 mm	0.019×10^{-15}	5.16	Infrared (5940 – 10,000A)
Nylon	Aluminum	0.015×10^{-7}	3.5	Infrared (5940 – 10,000A)

DURATION OF IMPACT FLASH

In previous discussion, only the peak luminosity associated with impact flash and not the integrated total luminosity over the time of emission was considered. The next step is to determine the time of occurrence of

the flash with respect to moment of impact, and to relate the duration of the flash to the elapsed time of projectile penetration and crater formation.

Available references (for instance, Refs. 1, 10, 14) show that the behavior of the projectile and the mechanism of the crater's formation vary, depending upon such factors as the velocity of impact and the relative strength of the specific projectile-target combination. It was suspected, therefore, that the initial peak luminosity was associated with the penetration of the more-or-less-intact projectile, and the trailing off of the flash with the deformation of the projectile and the expansion of the crater. This hypothesis is consistent with the greatly increased duration of the flash with a granite target as compared to the shorter duration of the flash with a sand target; the instrumentation that is available has permitted a critical test of this by displaying the photomultiplier outputs on oscilloscopes and photographing the results. Several of these will be examined.

The variation of luminosity with time is shown for three typical impact conditions in Fig. 21. The case of a hard projectile striking a soft target is illustrated by the top trace of a steel sphere impacting a sand target. There are two distinct phases in the generation of the impact flash. A sharp peak appears first, lasting in this case less than a microsecond, and followed by a long, low-intensity tail lasting many microseconds. Records with a high-speed framing camera show that the impact flash begins almost as soon as the projectile contacts the target; the peak is thus associated with the initial phase of penetration and cratering. For the case in question, the peak lasts less than the time it takes the projectile to penetrate the target to a depth equal to its own diameter.

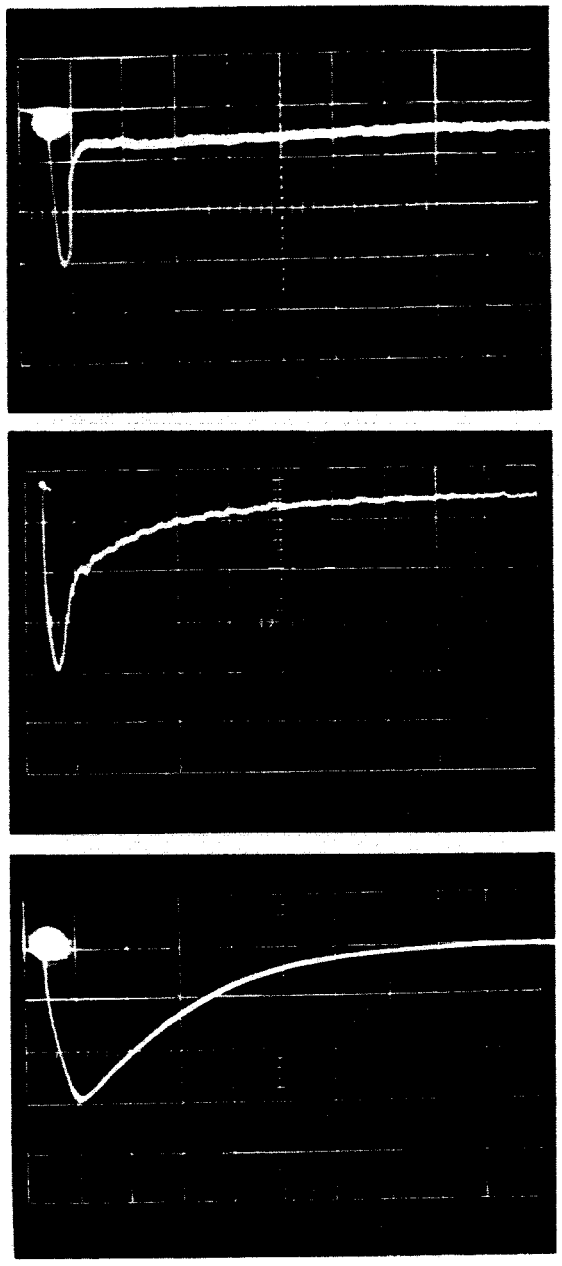

1/8-IN. DIAM. STEEL PROJECTILE
V = 8430 ft/sec
SAND TARGET

1/8-IN. DIAM ALUMINUM PROJECTILE
V = 7730 ft/sec.
SAND TARGET

1/8-IN. DIAM ALUMINUM PROJECTILE
V =8400 ft/sec
POLISHED GRANITE TARGET
(See Fig. 15)

SWEEP RATE = 1 μsec/cm

Fig. 21 Typical Photomultiplier Traces from Impacts of Various Projectile-Target Combinations

The case of an aluminum projectile striking a sand target is shown by the center trace. The first part of the peak lasts about the same time as that from the steel projectile. This initial peak is followed by a region in which the light decays from 0.5 to 0.1 of peak value in approximately 3 microseconds, perhaps because of the increased deformation of the aluminum projectile as compared with that of the steel projectile.

This point is borne out by the variation of luminosity with time as shown for the impact of an aluminum projectile into a granite target in the bottom trace. The entire peak region of the flash is now seen to be broadened. The time from the initial rise through the decay to 0.1 of peak value lasts nearly 5 microseconds. The case of aluminum into granite at 8,400 ft/sec begins to approach the fluid impact region; a crater is formed in the initial instance of impact, and material is jetted from the periphery of this initial crater at very high velocity.

Consequently, a surface of highly shocked material is exposed during the initial phase of cratering. The intensity of the shock is greatest at the beginning of impact, diminishing as the shock phenomena decrease with the increasing volume of material affected by the growing crater and expanding wave phenomena. The combination of these two effects produces the elongated shape of the light pulse seen in the case of aluminum into granite. In contrast to this, the case of steel into sand is probably close to the region of unbroken projectile impact, and the short light-pulse might indicate that highly shocked material is generated only during the moment of initial penetration. The case of aluminum into sand is probably an intermediate case somewhere between the unbroken projectile and the fluid impact cases.

Two additional experiments substantiate the fact that the luminosity occurs at the instant of impact and persists for only a very brief period. In the first experiment, the Beckman & Whitley high-speed framing camera was used to observe several projectile-target collisions. A typical framing sequence (Fig. 22) shows the projectile to have moved approximately 0.5 inch to impact the target, then the flash occurs in a single frame and is extinguished in a total time of less than 2.4 microseconds.

In the second experiment, which was aimed at demonstrating the short duration of the flash, 3/16-in. aluminum projectiles were fired at an average velocity of 17,600 ft/sec against different thicknesses of titanium sheets. Three thicknesses were tested – 0.012 in., 0.020 in., and 0.040 in. – and the measured peak luminosities were 523, 505, and 543 watts/steradian, respectively. These data show that the peak luminosity is unaffected by the thickness of the target and that the impact flash is produced on, or very near, the surfaces of the projectiles and the target (collision interface).

SPECTRUM OF AN IMPACT FLASH

To permit a more complete description of the phenomena of impact flash, it was necessary to observe the spectrum of the emitted radiation. From an analysis of the spectra obtained under varying conditions of impact, it is anticipated that the composition of an unknown target might be determined.

Only a few spectra have been observed to date, but the results are most interesting. Two typical spectrograms obtained from the impact of a nylon cylinder against both an aluminum and a sand target are shown in Figs. 23 and 24.

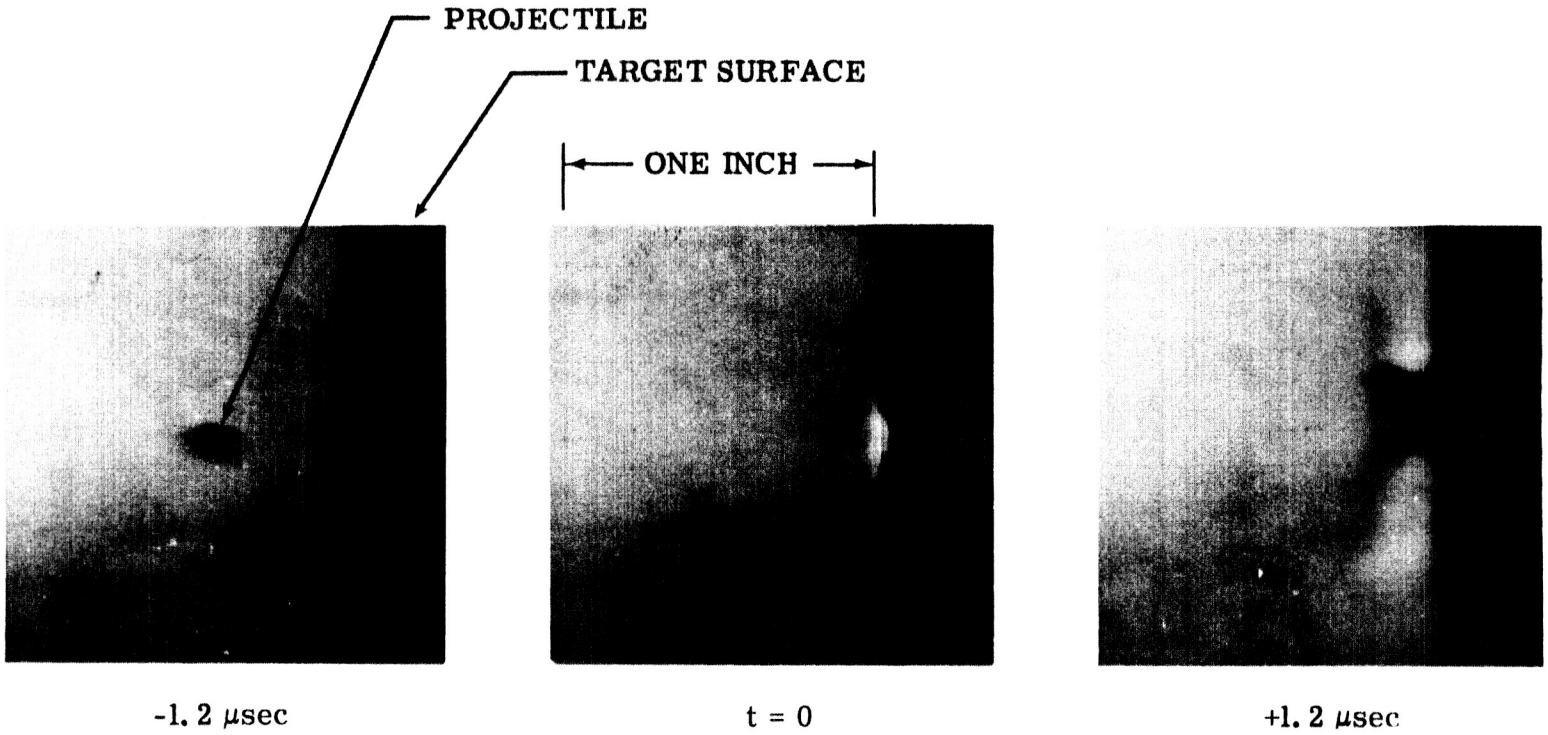

Fig. 22 Sequential Beckman-Whitley Photographs of a 1/8-In. Glass Sphere Impacting an Aluminum Target at 23,000 ft/sec

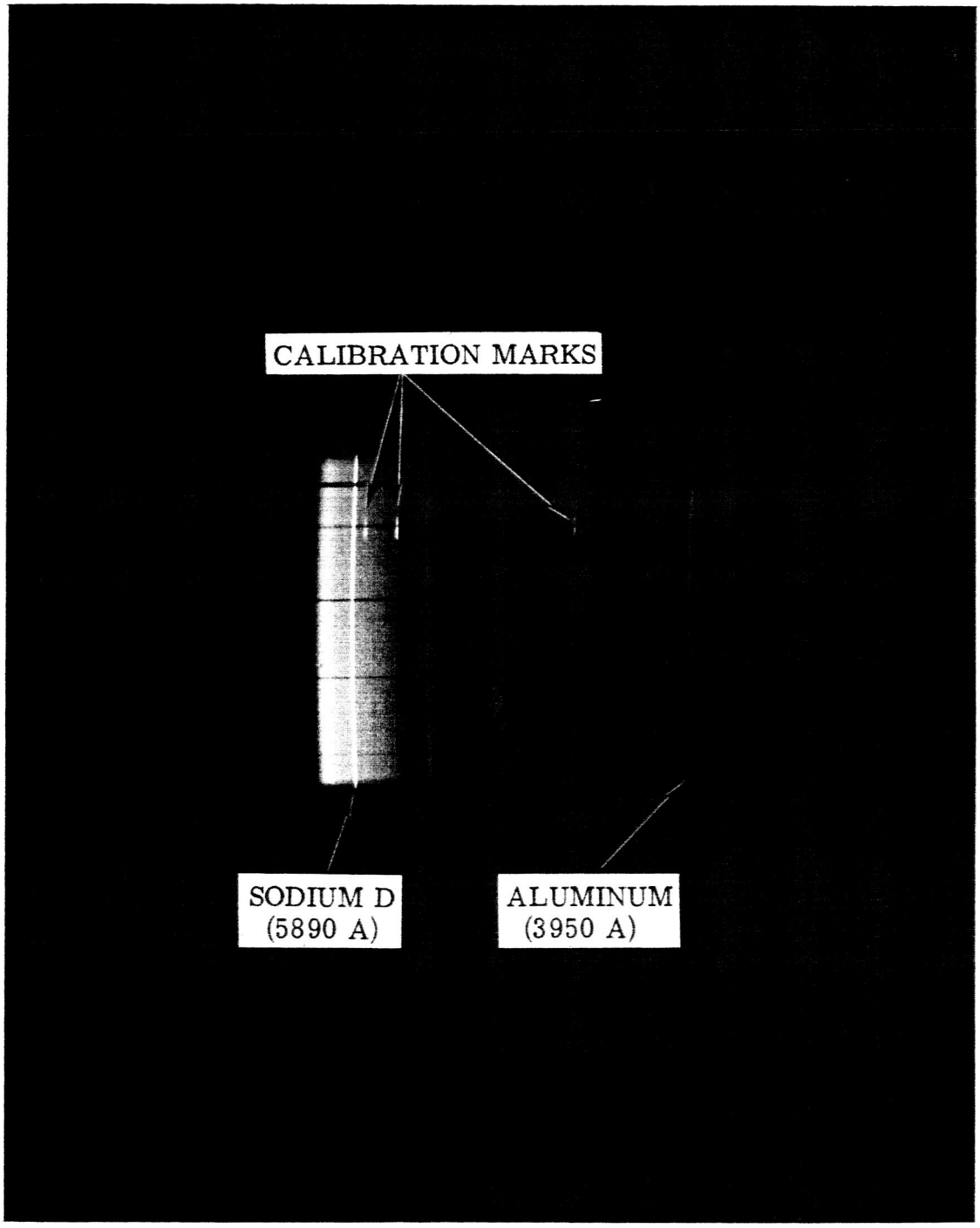

Fig. 23 Spectrogram of Impact Flash Generated by Nylon Cylinder Impacting an Aluminum Target at 24,600 ft/sec

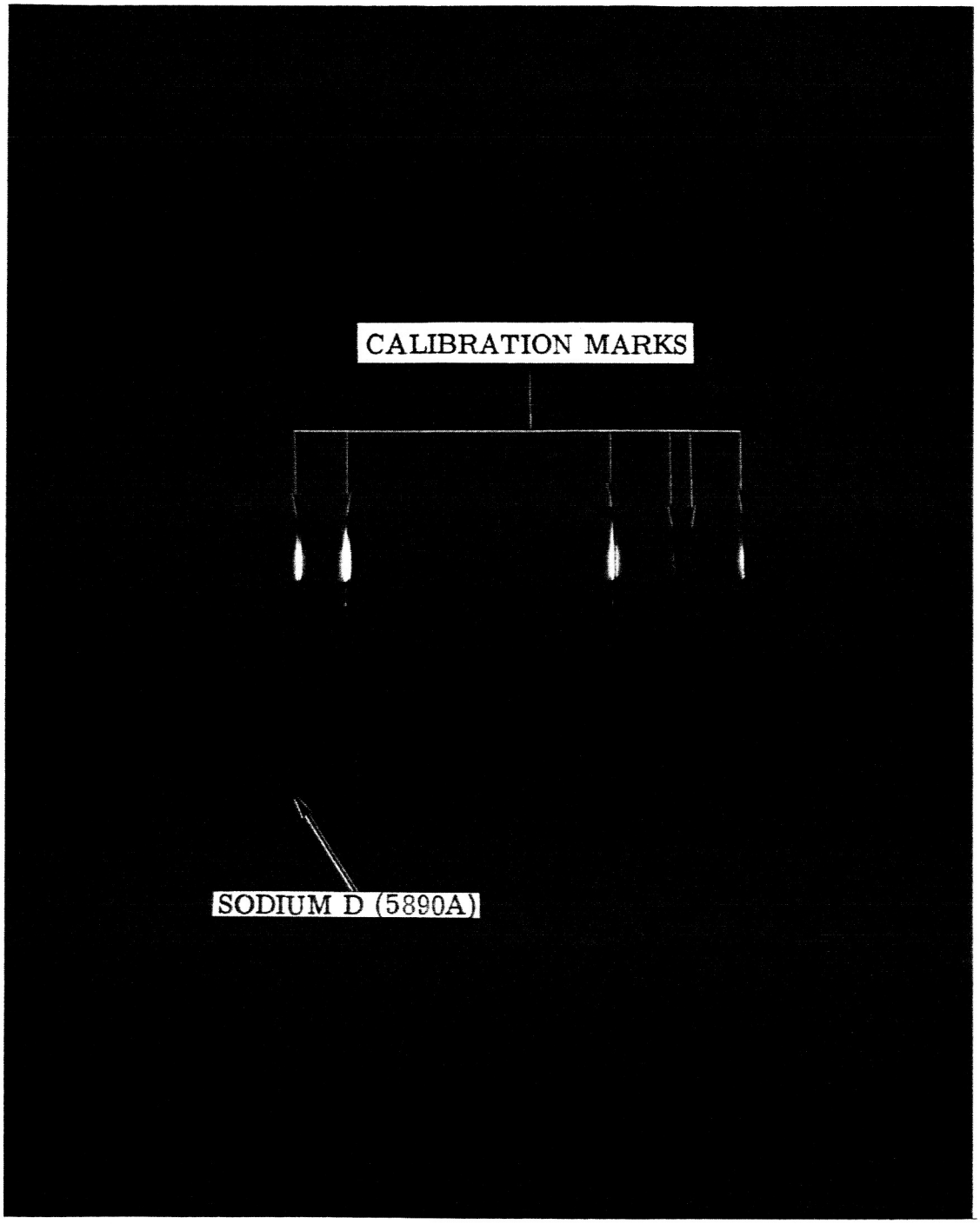

Fig. 24 Spectrogram of Impact Flash Generated by Nylon Spheres Impacting Sand Targets at Approximately 10,000 ft/sec (10 rounds superimposed)

Figure 23 is the result of the fairly intense flash generated by a nylon cylinder impacting an aluminum target at 24,600 ft/sec. The aluminum doublet at 3,950 Å appears in the near ultraviolet on the right side of the figure, and the aluminum oxide bands appear between the blue and the green. There is a continuum extending from the near infrared to the green, and the sodium D line appears strongly. (The short line segments are, of course, the image of a point-source mercury calibration which serves also to locate the point of impact along the vertical axis of the film.) The appearance of the aluminum oxide bands in the spectrum shown in Fig. 23 suggests an apparent anomaly when compared with the data of Figs. 12 and 13, which show the impact flash to be independent of the ambient gas and the surrounding gas pressure. It is believed, however, that the oxide bands appear as a result of surface oxidation on the unpolished surfaces of both projectile and target.

The second typical spectrograph (Fig. 24) is the result of the relatively weak flash generated by a nylon cylinder impacting a sand target at approximately 10,000 ft/sec. The intensity of the flash, so far below the demands of the spectrograph, made it necessary to superimpose the flash of ten successive rounds in order to obtain a legible record. Although the photographic quality of the resulting spectrograph leaves much to be desired, it seems clear that no line spectrum is generated – rather, there is a continuum in the near infrared. On the basis of Fig. 24, it would be difficult to determine the atomic and molecular composition of a sand target, for the line and band spectra may be present but too weak to be discernible. Further measurements with a more sensitive instrument are needed to investigate this possibility.

SECTION IV
DISCUSSION OF EXPERIMENTAL RESULTS

Referring to the data given in Figs. 12—20, the luminosity-versus-time plots of Fig. 21, and the empirical relationship given in Eq. 1, the observed phenomena can now be defined.

The appearance of an intense flash of light upon impact results from the conversion of mechanical energy to light. Most certainly, the energy of the projectile is expended in a number of possible reactions: heat is generated, radiation is emitted (possibly over the spectrum from gamma rays to microwaves), and mechanical work is done in forming the impact crater. (These experiments, however, were concerned with monitoring only that portion of the projectile energy which appears as visible light.) It is reasonable to assume that the magnitude of radiated visible light will be a function of the energy of the impacting projectile.

Since the target reacts to the impact in a manner dictated by the magnitude of the pressure pulse, it may also be reasonable to relate the intensity of impact flash to the properties of the materials after being shocked by the collision. Since a process by which luminosity is derived from the rapid application of pressure is unknown, a causal relationship between impact-generated pressure and luminous radiation cannot be established by these experiments. More complex, and much more difficult to define, are the excitation energy of atoms

under compression, and the multiple-electron problem created by the many possible ways in which electrons of different binding energies may react. Therefore, the present analysis is restricted to the establishment of an empirical relationship (Eq. 1) to describe the phenomena and to estimate the intensity of impact flash.

OBSERVATIONS OF LUNAR IMPACT

In applying the results of laboratory tests to observations of lunar impact by instruments on the earth, two cases will be considered: (1) the crash-landing of a Ranger lunar probe at lunar escape velocity, and (2) the impact of a marble-sized meteroroid. The question is whether or not a discernible record of the impacts of these objects can be obtained from the accompanying flash of light.

The answer to this question is critically dependent upon the design and sensitivity of the recording instrument. A full treatment of the subject is beyond the scope of this paper, and the discussion will be restricted to a limited study of two examples. The intent here is to present a method of analysis and to give a rough indication of possible answers.

Any earth-placed instrument will "see" the flash of a lunar impact. However, the identification of this flash will depend upon whether or not it can be distinguished from the noise on the record that represents the background intensity of the lunar surface. The first step in the analysis, then, is to obtain an estimate of this lunar background intensity.

In computing the lunar background intensity, only the positions of conjunction (moon and sun in the same direction from the earth – dark of the moon) and opposition (moon and sun in opposite directions from the earth – full moon) will be analyzed. In opposition, the moon is illuminated by light from the sun with an irradiance of 140 watts/sq ft (Ref. 15).

Considering a small, flat, diffuse area of lunar surface, it is easily seen that the intensity of reflected light along a normal to the surface is

$$I_N = \frac{\bar{a}\, I_R}{2\pi} \quad \ldots\ldots\ldots\ldots\ldots\ldots \quad (2)$$

where $\bar{a}$ is a normal albedo which may be taken as approximately 0.1. Substitution into this equation establishes the luminous intensity of the moon to be 2.2 watts/sterad-sq ft when the surface is in full sunlight (opposition). By a similar analysis, it can be established that when the moon is illuminated only by light reflected from the earth (conjunction), the solar irradiance is decreased to about 0.002 watts/sq ft, giving a reflected intensity of 3.0×10^{-5} watts/sterad-sq ft. Thus, part of the problem is to establish the possibility of observing a given impact flash against this background radiation.

The next step in the analysis is to estimate the intensity of the impact flash. The Ranger lunar probe is taken to be a vehicle of aluminum with a projected area of 19.6 sq ft, an effective length of 2 ft, and an impact velocity of 8,000 ft/sec. The lunar surface may be either sand or granite. The intensity of the flash is calculated from Eq. 1 using Table IV.

The effective duration of the flash, $\bar{t}$, is estimated to be the time it takes the probe to travel one-half its length; $\bar{t}$ is used to compute the total light from relation

$$\int I_n dt = I_{np} \bar{t} \quad \ldots \ldots \ldots \ldots \ldots \ldots \quad (3)$$

The results of these estimates are summarized in Table V.

Table V

PREDICTED IMPACT FLASH FOR RANGER LUNAR PROBE

Surface	I_{np} watts/sterad	$\bar{t}$ sec	$\int I_n dt$ watt-sec/sterad
Sand	1.1×10^5	1.3×10^{-4}	14
Granite	1.6×10^6	1.3×10^{-4}	200

The meteoroid may be either stone or iron and will be approximated by glass (for stone) and steel (for iron). Since the experimental data have been derived from a sand target with glass and steel projectiles, estimates of the impact flash can be made only for a lunar surface of sand. The meteoroid is taken to be a sphere 1/2-inch in diameter striking at 78,000 ft/sec.

Table VI

PREDICTED IMPACT FLASH FOR 1/2-IN. METEOROID

Type	Surface	I_{np} watts/sterad	$\bar{t}$ sec	$\int I_n dt$ watt-sec/sterad
Stone	Sand	1.2×10^9	0.3×10^{-6}	330
Iron	Sand	1.7×10^9	0.3×10^{-6}	450

The next step requires specification of the observing instrument. The two examples considered here are telescopes equipped with (1) a movie camera and (2) a photocell that measures the intensity of light. In example (1), continuous observation can be made by using two cameras, one recording while the other changes film.

The performance of either instrument will depend upon its sensitivity and on the signal-to-noise ratio. The question of sensitivity involves an analysis of instrument design that is too lengthy for this discussion. The signal-to-noise ratio also depends on the design of the instrument, but it is possible to treat this subject broadly for classes of instruments which depend upon the physical quantity measured. Leaving the question of sensitivity to be answered separately, certain conclusions concerning the possibility of observing the impact can then be drawn.

For the example of the telescope equipped with a movie camera, the impact flash will be recorded by a darkening of the film caused by an increase in light at the point of impact. The question, then, is whether or not the dark "spot" can be distinguished from the background. The contrast between the spot and the background on the negative will depend on the ratio of the total lumens produced by the flash to the lumens falling on a corresponding area of the background during the exposure time, Δt, of the camera. The signal-to-noise ratio is determined by the ratio,

$$\frac{\text{signal}}{\text{noise}} = \frac{\int I_{np} dt}{I_N \sigma A \Delta t} \quad \ldots\ldots\ldots\ldots\ldots \quad (4)$$

where I_N is the intensity of light from the lunar surface, and A is the area of the moon's surface that corresponds to the area of the impact flash. If the flash area is smaller than the minimum resolvable area of the instrument – considered to be the case here – the correct area to take is believed to be this minimum resolvable area,

$$\sigma A = \frac{\pi}{4} \left(\frac{5}{4} \frac{\lambda}{d} R\right)^2 \quad \ldots\ldots\ldots\ldots \quad (5)$$

where λ = wavelength of the light

d = aperture of the telescope

R = distance from the earth to the moon

Considering a telescope with an aperture of 12 inches and taking green light as representative, $\lambda = 2 \times 10^{-5}$ inches. Under these conditions, $A = 5 \times 10^6$ ft^2.

Considering also that the exposure time of the movie camera attached to the telescope is 0.1 second,

$$\Delta t = 0.1 \text{ sec.}$$

Now the signal-to-noise ratio for various conditions of impact being investigated can be determined. This ratio is given in Table VII.

Table VII

OBSERVATION OF LUNAR IMPACT WITH TELESCOPE

Lunar Surface	Object	Signal/Noise Full Moon	Signal/Noise Dark Moon
Sand	Ranger probe	0.00002	1.3
Granite	Ranger probe	0.00026	19.1
Sand	Stone meteoroid	0.00043	31.4
Sand	Iron meteoroid	0.00058	42.8

Table VII shows that on the basis of signal-to-noise ratio, a 12-inch telescope with a 0.1-second-exposure camera will not produce a discernible record of the flash from the impact of either the Ranger probe or a 1/2-inch meteoroid on the bright side of the moon (at full moon). On the other hand, there is the distinct possibility that a record could be made of the impact of either the probe or a meteoroid on the dark side of the moon (at opposition). Whether or not a photographic record could actually be made will depend upon questions of sensitivity and other factors which include frequency of occurrence in the case of meteoroids. This is a subject for future investigation.

For the example of the telescope equipped with a photocell for continuous monitoring of the total light received by the telescope, the peak intensity of the impact flash will increase the background signal produced by the light received from the lunar surface. This background signal will depend on the angle of view of the telescope as determined by the area of the moon's surface to be observed, A_o. The signal-to-noise ratio is thus given by

$$\frac{\text{signal}}{\text{noise}} = \frac{I_{np}}{I_N A_o} \quad \ldots\ldots\ldots\ldots\ldots\ldots \quad (6)$$

For this example, the angle of view will be selected arbitrarily as two minutes of arc, which corresponds to a circular surface on the moon with a diameter of 135 miles and an area of 3.9×10^{11} sq ft. The signal-to-noise ratios for the various conditions of impact are listed in Table VIII.

Table VIII

OBSERVATION OF LUNAR IMPACT WITH PHOTOCELL

		Signal/Noise	
Lunar Surface	Object	Full Moon	Dark Moon
Sand	Ranger probe	1.3×10^{-7}	1.0×10^{-2}
Granite	Ranger probe	1.9×10^{-6}	1.4×10^{-1}
Sand	Stone meteoroid	1.4×10^{-3}	1.1×10^{2}
Sand	Iron meteoroid	2.0×10^{-3}	1.4×10^{2}

Table VIII gives much the same information as Table VII. Impacts on the bright surface of a full moon could not be distinguished from the background. On the other hand, the impact of a meteoroid on the dark side would be visible against the background noise. This estimate supports the observations of Ref. 7. In contrast to the previous example, however, the 2-minute telescope could not "see" the impact of the Ranger probe even on the dark moon.

There is one obvious improvement in technique which should be mentioned, since it may have a bearing on the conclusions drawn from these estimates of the performance of the 2-minute telescope with continuous photocell monitor. The duration of the flash is very short, lasting only about 0.1 millisecond in the case of the Ranger probe. This suggests that the photocell circuit should be provided with a filter passing only high-frequency signals (above 1,000 cycles per second). The background signal should be greatly reduced by this technique, and the signal-to-noise ratio improved accordingly. Again, the improvement realized in this manner is a subject for future investigation.

SECTION V
CONCLUSIONS

Although there is only limited data on the phenomena of impact flash and, more important, no definitive theory to relate the generation of a flash to the mechanics of impact, certain conclusions may be drawn concerning the possibility of observing impacts of meteoroids and space probes on the lunar surface.

(1) In the experimental program described, in all cases of impact above velocities of about 5,000 ft/sec, an impact flash was observed regardless of projectile or target material.

(2) Although tests were conducted only with air at pressures ranging from 0.0014 to 760 mm Hg, and with helium at pressures of 0.004 and 760 mm Hg, there appears to be no significant effect of the composition or pressure of the gas surrounding the impact area on the magnitude of the impact flash. This being the case, it is highly probable that a flash will occur in the case of a lunar impact at a velocity greater than 6,000 ft/sec.

(3) An empirical fit of the luminosity data indicates that the peak luminosity varies with the projected area of the projectile and with a power of the velocity that ranges between 3 and 9. The constant of proportionality between the peak luminosity and the product of the projectile area with a power of the impact velocity depends primarily on the materials of the target.

(4) Examination of high-framing-rate camera records and photocell records shows that the flash starts at the first contact of the projectile with the target and rises to peak value during the first part of the impact process. The flash appears to be closely associated with material that is highly shocked in the initial phase of impact. The time duration of the flash varies markedly with changes in the materials of both projectile and target, particularly the latter.

(5) The spectrograms indicate that only a continuum, rather than a distinct atomic line spectra, is obtained under conditions of impact on sand targets below 10,000 ft/sec.

(6) To record the impact of a space probe or a meteoroid on the surface of the moon by observations made from the earth, a very limited study indicates the possibility of doing so if the impact takes place on a "dark" moon (illuminated by earthshine only). But if the impact occurs on the bright surface of a full moon, recording the impact would appear to be a most difficult task unless the monitoring photocell is equipped with a high-frequency bandpass filter or other signal-processing circuitry to reduce the background noise.

REFERENCES

1. A.C. Charters, "High Speed Impact," Sci. American, Oct 1960

2. Royal Aircraft Establishment, On Phenomena Observed at the Instant of Impact of the Second Soviet Cosmic Rocket on the Moon, by O.B. Dluzhnevskaya, ASTIA No. 253914, Feb 1961

3. P.S. Epstein, "What is the Moon Made Of?," Phys. Rev., Vol. 33, 1929, p. 269

4. A.J. Wesselink, "Heat Conductivity and Nature of the Lunar Surface Material," Bull. Aston. Inst., Neth., Vol. 10, 1948, pp. 350 – 363

5. J.C. Jaeger and A.F.A. Harper, "Nature and Surface of the Moon," Nature, Vol. 166, 16 Dec 1950, p. 1026

6. T. Gold, "The Lunar Surface," J. Roy. Astron. Soc., Vol. 115, No. 6, 1955

7. Aviation Week, Vol. 76, No. 10, 5 Mar 1962, p. 70

8. W.W. Atkins, "Flash Associated with High Velocity Impact on Aluminum," J. Appl. Phys. Vol. 26, 1955

9. W.H. Clark, R.R. Kadisch, and R.W. Grow, "Spectral Analysis of the Impact of Ultra Velocity Copper Spheres into Copper Targets," Tech. Report OSR-16, University of Utah, 1 Sep 1959

10. W.C. Maurer and J.S. Rinehart, "Impact Crater Formation in Rock," Proc. 4th Symposium on Hypervelocity Impact, APGC-TR-60-39, Eglin AFB, Florida, Sep 1960

11. H.J. Moore, R.V. Tugu, and D.E. Gault, "The Geology of Hypervelocity Impact Craters," (paper presented at 5th Symposium on Hypervelocity Impact, Denver, Nov 1961); B. Pat Denardo,

"Measurements of Momentum Transfer from Plastic Projectiles to Massive Aluminum Targets at Speeds up to 25,600 ft/sec," NASA Tech. Note d-1210, Mar 1962; D.E. Gault "Change in Lunar Characteristics by Micrometeoroids and the Shape and Size of Particles," and E.M. Shoemaker, "Size Frequency Distribution of Small Primary and Secondary Impact Craters," Proc. Lunar Surface Materials Conf., Boston, Massachusetts, May 1963; see also R.W. MacCormack, "Investigation of Impact Flash at Low Ambient Pressures" (paper presented at Sixth Symposium on Hypervelocity Impact, Cleveland, Ohio, 1 May 1963)

12. R.B. Baldwin, The Face of the Moon, The University of Chicago Press, Chicago, Illinois, 1949; see also T. Gold, "Structure of the Moon's Surface" (paper presented at Lunar Surface Materials Conf., Boston, May 1963)

13. A.C. Charters, "The Free Flight Range: A Tool for Research in the Physics of High Speed Flight," ARS Preprint 1986-61 (paper presented at the International Hypersonics Conference, MIT, Aug 16 – 18, 1961)

14. J.W. Gehring, "Observations of the Phenomena of Hypervelocity Impact," Proceedings of the 4th Symposium on Hypervelocity Impact, APGC-TR-60-39, Vol. II, Eglin Air Force Base, Florida, Apr 1960. Also R.J. Eichelberger and J.W. Gehring, "Effects of Meteoroid Impact on Space Vehicles," ARS J., Vol. 32, No. 10, Oct 1962

15. Gilbert Fielder, Structure of the Moon's Surface, Pergamon Press, New York, 1961; Satellite Environment Handbook, Stanford University Press, 1961; E.J. Opik, "The Density of the Lunar Atmosphere," Irish Astron. J., Vol. 3, 1955, pp. 137 – 143